Robotica (2022), **40**, pp. 520–543
doi:10.1017/S0263574721000667

CAMBRIDGE
UNIVERSITY PRESS

RESEARCH ARTICLE

Communication-free autonomous cooperative circumnavigation of unpredictable dynamic objects

A. S. Matveev[1,2]* and V. V. Magerkin[1]

[1]Department of Mathematics and Mechanics, Saint Petersburg University, Universitetskii 28, Petrodvoretz, St.Petersburg 198504, Russia and [2]Faculty of Control Systems and Robotics, ITMO University, 49 Kronverksky Pr., St. Petersburg 197101, Russia
*Corresponding author. Email: almat1712@yahoo.com

Received: 19 January 2021; **Revised:** 4 May 2021; **Accepted:** 4 May 2021; **First published online:** 9 June 2021

Keywords: autonomous sensor-based reactive navigation, multirobot scenario, unpredictably moving curve, curve tracking, effective self-deployment, global convergence

Abstract
Each of several speed-limited planar robots is driven by the acceleration, limited in magnitude. There is an unpredictable dynamic complex object, for example, a group of moving targets or an extended moving and deforming body. The robots should reach and then repeatedly trace a certain object-dependent moving and deforming curve that encircles the object and also achieve an effective self-deployment over it. This may be, for example, the locus of points at a desired mean distance or distance from a group of targets or a single extended object, respectively. Every robot has access to the nearest point of the curve and its own velocity and "sees" the objects within a finite sensing range. The robots have no communication facilities, cannot differentiate the peers, and are to be driven by a common law. Necessary conditions for the solvability of the mission are established. Under their slight and partly unavoidable enhancement, a new decentralized control strategy is proposed and shown to solve the mission, while excluding inter-robot collisions, and for the case of a steady curve, to evenly distribute the robots over the curve and to ensure a prespecified speed of their motion over it. These are justified via rigorous global convergence results and confirmed via computer simulations.

1. Introduction

Over the past decades, the formation control has become a mature discipline [1, 2], and its focus has been much shifted to the decentralized and distributed control paradigm and the issue of communication and sensorial limitations. This focus brings strong analytical challenges [1] and makes rigorous nonlocal convergence analysis a difficult task, though some rigorous results have been yet obtained.

In this area, much effort has been devoted to the problem of autonomously driving multiple planar robots into a formation encircling a targeted object, see, for example, refs. [3, 4, 5, 6, 7, 8, 9, 10, 11, 12, 13, 14, 15, 16]. A motivation of this problem comes from many sources, including rescue operations, transportation of large objects, exploration and surveillance, minimization of security risks, deployment of mobile sensor/actuator networks [17], escorting and patrolling missions, troop hunting, etc. Within this diversity, the targeted object has various incarnations; for example, this may be a single body or a group of them, the concerned body can be treated as a point in some cases and, in other situations, should be viewed as a one- or two-dimensional entity, moving and deforming in general.

In such missions, the robots should approach the object and arrive at tactically advantageous positions. The locus of such positions is often an object-dependent curve, for example, a circle centered at a point-wise target, or the set of points equidistant from the edges of an extended object, or the locus of points at a given mean distance from a group of targets, etc. After arrival at this curve, the robots should repeatedly trace it. Since their speeds normally exceed that of the object, the result is moving around it, which gives rise to the term *circumnavigation*. Typically, the robots should also distribute themselves on the curve so that the robotic team surrounds the targeted object more or less uniformly.

Up to now, research on robotic circumnavigation was mostly focused on point-wise targets. A single moving target with access to its velocity vector and fully actuated robots are treated in ref. [8]. Hilare-type robots are considered in ref. [15], and an evidence of the team's local stability is offered. Assuming that the target obeys a known escaping rule, [14] gives conditions under which a linear control law drives identical linear agents with full actuation and observation into a target-centric formation. The cyclic pursuit pattern is used in ref. [7] to ensure capturing a moving target in 3D at a given altitude provided that there is an access to the target's velocity vector, like in ref. [8]. For a steady target, basic findings of ref. [7] are extended to stable identical underactuated vehicles in ref. [6].

The cyclic-pursuit paradigm assumes a steady ring-like information-flow graph. More general graphs are treated in ref. [5] for a moving target with the measured velocity vector. In refs. [9, 18], research similar to ref. [5] is reported, with assuming uncertainties in data on the target [9] or transmitted information [18] and access of every robot to the velocities and accelerations of the neighbors. In these works, the information flow is independent of the robots' motion. A more realistic situation is examined in ref. [4], where every robot observes its angular predecessor and follower in the circular order around a moving target. Whereas the above papers assume an unlimited range of visibility, [3] handles a realistic case of a finite range, and shows that the proposed control law ensures local stability of the uniform formation around a steady target, though no rigorous global convergence results are provided. An unpredictably moving speedy target and speed- and acceleration-limited robots with a finite sensing range are studied in ref. [19], where it is proved that the proposed decentralized control law drives the robots to a given distance to the target and ensures their even distribution over the respective moving circle, along with a desired common angular velocity of rotation about the target.

To the best of the author's knowledge, circumnavigation of multiple unknown targets was studied only for point-wise ones and a single pursuer. In ref. [20], the simple-integrator robot is driven to and then along a circle centered at the mean of the targets' positions if the targets are steady; otherwise, there is an error proportional to their speed. For a Dubins-car-like robot, the controller from ref. [21] drives the mean distance to speedy targets to a given value. In ref. [22], a similar result is obtained in the case where the mean distance is replaced by the distance to the nearest target. As for extended targets, circumnavigation of a steady 2D body by Dubins-car-like robots and their even self-distribution around it at a given distance is treated in ref. [23], encircling an arbitrarily moving and deforming object by a single such a robot is studied in ref. [24]. In both papers, the control laws are justified by global convergence results.

Meanwhile, many issues remain open in the discussed research field. For example, circumnavigation of dynamic extended objects by many robots lies in an absolutely uncharted territory, irrespective of whether the object is single or multiple; the same is true for multiagent circumnavigation of many moving point-wise targets. This paper aims at filling these gaps. The main idea behind it is to offer a solution to a core problem that must be inevitably solved in the majority of the concerned circumnavigation missions, including the mentioned poorly addressed ones.

Specifically, we consider an unpredictably moving and deforming Jordan curve. It is treated as a self-sufficient component of the environment, though this curve is typically inferred from a targeted object, either single or complex, and is the locus of the preferable locations relative to the object. There is a team of point-wise robots, each driven by the acceleration vector. This vector and the robot's velocity are upper bounded in magnitude. In its local frame, every robot identifies positions of the objects within a finite sensing range, the nearest point of the curve, the direction of its own velocity, and the tangential speed relative to the curve. It cannot assess the speeds of other objects or distinguish between the peers and has no communication facilities. The robots should approach and then trace the moving curve, while achieving an effective self-distribution over it.

We disclose conditions necessary for the mission to be feasible. Then we present a decentralized and distributed control law that solves the mission and excludes collisions among the robots under only a slight enhancement of those conditions. These are shown via a rigorous global convergence result and confirmed by computer simulation tests. The proposed law is hybrid: it combines event-based switching among discrete modes with nonlinear switching regulation within every mode. Furthermore, this law is computationally inexpensive and reactive, that is, it directly converts the current observation into the current control, and yet exhibits the capacity for guaranteed global convergence.

The body of the paper is organized as follows. Section 2 describes the problem. Section 3 offers necessary conditions for the mission feasibility and assumptions. The control law and main results are presented in Sections 4 and 5, respectively. Section 6 reports on computer simulation tests, and Section 7 offers brief conclusions. All proofs are placed in appendices.

2. Problem formulation

Every of N planar robots is driven by the acceleration limited in magnitude by a constant $\overline{a}$. The speeds of the robots do not exceed $\overline{v} > 0$. No robot distinguishes between the partners and has communication facilities. In its local frame, any robot can identify the direction of its own velocity and has access to the relative coordinates of the objects within a finite sensing range. The plane also hosts a moving and deforming Jordan curve $\Gamma = \Gamma(t)$, which is unknown, unpredictable, and maybe, speedy. The robots should reach this curve and then trace it in a common given direction. An effective self-distribution over Γ should be achieved, with the even one being an ideal option. In its local frame, any robot can determine its own *projection* onto Γ (i.e., the nearest point of Γ) and so find the distance to Γ. The robot also can figure out whether it lies inside Γ or not, as well as its own speed in the direction parallel to Γ. Some examples of pertinent missions are as follows.

(1) There is a moving 2D continuum $D(t) \subset \mathbb{R}^2$ of arbitrary and time-varying shape. This covers scenarios with reconfigurable rigid bodies, forbidden zones between vehicles moving in a platoon, flexible obstacles, like fishing nets or schools of fish, virtual obstacles, like areas contaminated with chemicals, or online estimated areas of threats. The robots should advance at a given distance $d_0 > 0$ to $D(t)$, then maintain it, circumnavigate $D(t)$ in a common direction, and form a dynamic envelope of $D(t)$ via uniformly surrounding $D(t)$. In this case, $\Gamma(t)$ is the locus of points at a distance of d_0 from $D(t)$. The capacity to determine the closest point of $\Gamma(t)$ follows from the similar capacity with respect to $D(t)$: the former point results from the latter via its shift by d_0 toward the robot.

(2) There are multiple speedy and unknowingly moving pointwise targets $\boldsymbol{p}_j(t)$. It is needed to drive the root mean square distance d_{mean} from every robot to the targets to a given value d_0, to effectively distribute the robots over the locus $\Gamma(t)$ of points with $d_{\text{mean}} = d_0$, and to subsequently follow the targets with maintaining this value and distribution. The capacity to determine the closest point of $\Gamma(t)$ arises from access to the positions of the targets.

(3) In the case 2, the targets should be fully enclosed and tightly circumnavigated: a given distance d_0 to the currently nearest target should be reached and maintained by every robot, while all targets are to be inside its path. In this case, $\Gamma(t)$ is composed of arcs of d_0-circles $\{\boldsymbol{r} \in \mathbb{R}^2 \colon \min_i \|\boldsymbol{r} - \boldsymbol{p}_i(t)\| = d_0\}$ centered at the targets, where $\|\cdot\|$ is the standard Euclidean norm. The targets are assumed not to spread too far apart from each other so that such arcs can be concatenated to form a nonself-intersecting loop $\Gamma(t)$ encircling all targets. Since this curve is typically nonsmooth, whereas the robots can trace only smooth paths with nonzero speeds, $\Gamma(t)$ should be approximated by a smooth curve to make the mission feasible; see ref. [22] for details.

Let $\boldsymbol{r}_i$ stand for the absolute position of the ith robot. We model this robot as a double integrator

$$\ddot{\boldsymbol{r}}_i = \boldsymbol{a}_i, \quad a_i := \|\boldsymbol{a}_i\| \leq \overline{a}, \quad \boldsymbol{r}_i(0) = \boldsymbol{r}_i^0, \quad \boldsymbol{v}_i(0) = \boldsymbol{v}_i^0, \quad \|\boldsymbol{v}_i^0\| \leq \overline{v}. \tag{1}$$

Here $\boldsymbol{v}_i$ is the robot's velocity, its acceleration $\boldsymbol{a}_i$ is the control, and $\|\boldsymbol{w}\| := \sqrt{\langle \boldsymbol{w}; \boldsymbol{w}\rangle}$ and $\langle \cdot ; \cdot \rangle$ are the Euclidean norm and inner product, respectively. The first equation in (1) is in effect if the speed

https://doi.org/10.1017/S0263574721000667 Published online by Cambridge University Press

$v_i := \|\boldsymbol{v}_i\| \leq \overline{v}$. The controller design must meet this bound, which permits us not to discuss what may happen above the bound or under a trespass attempt.

To describe the dynamic curve $\Gamma(t)$, we use the Lagrangian approach [25] and so introduce a *reference configuration* $\Gamma_* \subset \mathbb{R}^2$ and a time-varying *configuration map* $\Phi(\cdot, t)$ that transforms Γ_* into the *current configuration* $\Gamma(t) = \Phi[\Gamma_*, t]$. We limit the motion of $\Gamma(t)$ by only few and minimal conventions, typical for the general continuum mechanics [25].

Assumption 2.1. *The set Γ_* is a C^3-smooth Jordan curve; $\Phi(\cdot)$ is defined on an open connected vicinity O_* of Γ_*, is C^3-smooth and one-to-one, its Jacobian matrix is everywhere invertible.*

The velocity and acceleration of the moving "particle" $\boldsymbol{q} = \boldsymbol{q}(t) \in \Gamma(t)$ are given by $V(\boldsymbol{q}, t) := \frac{\partial \Phi}{\partial t}[\boldsymbol{q}_*, t]$ and $A(\boldsymbol{q}, t) := \frac{\partial^2 \Phi}{\partial t^2}[\boldsymbol{q}_*, t]$, where $\boldsymbol{q}_* \in \Gamma_*$ is the "seed" of the point $\boldsymbol{q}(t) = \Phi(\boldsymbol{q}_*, t)$. We use the following notations:

- $\boldsymbol{\varrho}_i(t) := \pi[\boldsymbol{r}_i(t), t]$, where $\pi(\boldsymbol{r}, t)$ is the *projection* of $\boldsymbol{r}$ onto $\Gamma(t)$ (point of $\Gamma(t)$ nearest to $\boldsymbol{r}$);
- $d_i(t)$, signed distance from robot i to $\Gamma(t)$, positive from outside;
- $\boldsymbol{w}^\perp$, vector $\boldsymbol{w}$ rotated through $+\pi/2$; positive angles are countered counterclockwise;
- $\boldsymbol{\tau}(\boldsymbol{\varrho}, t)$, unit vector tangent to $\Gamma(t)$ at $\boldsymbol{\varrho} \in \Gamma(t)$ and oriented counterclockwise;
- $\boldsymbol{n}(\boldsymbol{\varrho}, t) = \boldsymbol{\tau}(\boldsymbol{\varrho}, t)^\perp$, unit vector normal to $\Gamma(t)$;
- $W_\tau(\boldsymbol{\varrho}, t) := \langle W; \boldsymbol{\tau}(\boldsymbol{\varrho}, t) \rangle$, $W_n(\boldsymbol{\varrho}, t) := \langle W; \boldsymbol{n}(\boldsymbol{\varrho}, t) \rangle$, tangential and normal projections of W;
- $\dot{\mathfrak{s}}_i := \left\langle \dot{\boldsymbol{\varrho}}_i(t); \boldsymbol{\tau}[\boldsymbol{\varrho}_i(t), t] \right\rangle$, tangential speed of the projection $\boldsymbol{\varrho}_i(t)$;
- $\varkappa(\boldsymbol{\varrho}, t)$, signed curvature of the curve $\Gamma(t)$ at point $\boldsymbol{\varrho} \in \Gamma(t)$ at time t;
- $\omega(\boldsymbol{\varrho}, t) := \left\langle \frac{d\boldsymbol{\tau}[\pi(\boldsymbol{\varrho}, t+\theta), t+\theta]}{d\theta} |_{\theta=0}; \boldsymbol{n}(\boldsymbol{\varrho}, t) \right\rangle$, angular velocity at which Γ rotates at point $\boldsymbol{\varrho} \in \Gamma(t)$;
- $\epsilon(\boldsymbol{\varrho}, t) := \frac{d\omega[\pi(\boldsymbol{\varrho}, t+\theta), t+\theta]}{d\theta} |_{\theta=0}$, angular acceleration of the curve Γ at point $\boldsymbol{\varrho} \in \Gamma(t)$ at time t;
- $\wp(\boldsymbol{\varrho}, t) := \frac{d\varkappa[\pi(\boldsymbol{\varrho}, t+\theta), t+\theta]}{d\theta} |_{\theta=0}$, curvature change rate at point $\boldsymbol{\varrho} \in \Gamma(t)$ at time t;
- $\sigma = \pm 1$ gives the desired direction of tracing the curve Γ (counterclockwise/clockwise).

3. Necessary conditions and assumptions of theoretical analysis

To avoid assumptions that are high above the necessary level, we first disclose conditions that are necessary for the mission to be feasible. Our assumptions will be slight enhancements of these.

To regulate the output d_i to the desired value 0, *local controllability* of the output is classically required. At the least, this trait means that respective controls can cause keeping the distance to Γ constant, converging to Γ, and diverging from Γ. Since the relative degree of the output d_i is 2, this means that whenever $\dot{d}_i = 0$, the sign of $\ddot{d}_i$ can be arbitrarily manipulated by means of feasible accelerations. We assume this only at the maximal speed and everywhere in the *operational zone*. For the sake of convenience, this zone is delineated in terms of the distance d to Γ:

$$Z_{\text{op}} := \left\{(\boldsymbol{r}, t): d_- < d < d_+\right\}, \qquad \text{where} \quad d_- < 0 < d_+ \tag{2}$$

are given. By [26, Lemma 1], the capacity to just maintain the distance to Γ implies the following properties (up to a minor relaxation of the second of them).

Assumption 3.1. *At any time t and for any point $\boldsymbol{\varrho} \in \Gamma(t)$, the following inequality holds:*

$$0 < 1 + \varkappa(\boldsymbol{\varrho}, t) d_{-\operatorname{sgn} \varkappa}. \tag{3}$$

At any time, the distance from any point $\boldsymbol{r}$ of the operational zone (i.e., such that $(\boldsymbol{r}, t) \in Z_{\text{op}}$) to the curve $\Gamma(t)$ is furnished by a single point of this curve.

Assumption 3.1 implies that in Z_{op}, the projection $\pi(\boldsymbol{r}, t)$ not only is uniquely defined but also smoothly depends on $\boldsymbol{r}$ and t, and so is the distance $d = \|\boldsymbol{r} - \pi(\boldsymbol{r}, t)\|$ to $\Gamma(t)$ provided that $\boldsymbol{r} \notin \Gamma(t)$. For an arbitrary steady C^2-smooth Jordan loop Γ, Assumption 3.1 holds whenever d_+ and d_- are small enough.

https://doi.org/10.1017/S0263574721000667 Published online by Cambridge University Press

To complete discussion of the controllability, we omit the argument $(\boldsymbol{\varrho}, t)$ in $\varkappa, \omega, V_\tau, A_n$ and put

$$\gamma_\pm(d, \boldsymbol{\varrho}, t, \mathcal{V}) = \frac{\varkappa(\overline{v}^2 - \mathcal{V}^2) \pm 2\omega\sqrt{\overline{v}^2 - \mathcal{V}^2} - \omega^2 d}{1 + \varkappa d} - \varkappa V_\tau^2 - 2\omega V_\tau + A_n. \tag{4}$$

Lemma 1. *Suppose that Assumption 3.1 holds. The output d_i is locally controllable in Z_{op} when moving at the maximal speed if and only if for any time t, point $\boldsymbol{\varrho} \in \Gamma(t)$, and distance $d \in [d_-, d_+]$,*

$$|V_n| < \overline{v}, \qquad |\gamma_\pm(d, \boldsymbol{\varrho}, t, V_n)| < \overline{a}\sqrt{1 - V_n^2/\overline{v}^2}. \tag{5}$$

Regulation of the tangential $v_{i,\tau}$ and normal $v_{i,n}$ velocity is inherent in control of the inter-robot distance s along Γ and the distance d to Γ, respectively. The latter velocity imposes bounds on the former: $v_{i,\tau} \in \left[-\sqrt{\overline{v}^2 - v_{i,n}^2}, \sqrt{\overline{v}^2 - v_{i,n}^2} \right]$. In order that the two concerned outputs s, d be independently controllable, we demand that these bounds do not carry a potential for an insurmountable trend in the evolution of $v_{i,\tau}$: the gap between $v_{i,\tau}$ and the above both upper and lower bound can be driven to any direction via a feasible acceleration without prejudice to d_i-controllability whenever $\|\boldsymbol{v}_i\| < \overline{v}$. We request this only on the curve Γ, where the inter-robot distances join the set of primal concerns. Meanwhile, $v_{i,n}$ and $v_{i,\tau}$ are directly affiliated with the respective parts $a_{i,n}$ and $a_{i,\tau}$ of the control input $\boldsymbol{a}_i$. To keep the robot on Γ, these parts must balance the matching parts of the centripetal and Coriolis accelerations and the own acceleration of Γ. Hence, the distribution of the available control effort $\overline{a}$ over $a_{i,n}$ and $a_{i,\tau}$ is determined by the speeds and accelerations of the points of Γ, whose measurement or estimation usually represents a real challenge in practical setting. This motivates us to limit ourselves to control solutions that do not call for resolving this challenge and are based on a situation-independent allocation of the control effort. To summarize, we denote the afore-discussed gap by

$$g_{\pm,i} := v_{i,\tau} \pm \sqrt{\overline{v}^2 - v_{i,n}^2}. \tag{6}$$

Definition 1. The robot is said to be *locally controllable on Γ with situation-independent allotment of the control effort* if there are $\overline{a}_\tau, \overline{a}_n > 0$ such that $\overline{a}_\tau^2 + \overline{a}_n^2 \le \overline{a}^2$ and whenever the robot goes on Γ and $v_i < \overline{v}$, the following holds:

(1) The signs of $\ddot{d}_i$ and $\dot{g}_{\pm,i}$ (with any sign drawn from $\pm$) can be freely manipulated via normal $a_i^n \in [-\overline{a}_n, \overline{a}_n]$ and tangential $a_i^\tau \in [-\overline{a}_\tau, \overline{a}_\tau]$ accelerations, respectively, if the other acceleration lies in the indicated interval.

Lemma 2. *If the controllability described in Definition 1 holds, then there exist $\overline{a}_\tau, \overline{a}_n > 0$ such that $\overline{a}_\tau^2 + \overline{a}_n^2 \le \overline{a}^2$, (5) is true with $\overline{a} := \overline{a}_n, d = 0, < \mapsto \le$, and for any time t and point $\boldsymbol{\varrho} \in \Gamma(t)$,*

$$\left|\omega^2/\varkappa + \varkappa V_\tau^2 + 2\omega V_\tau - A_n\right| < \overline{a}_n \quad \text{whenever} \quad |\omega| < |\varkappa|\sqrt{\overline{v}^2 - V_n^2}, \tag{7}$$

$$2\left[|\omega| + |\varkappa|\sqrt{\overline{v}^2 - V_n^2}\right]|V_n| + \overline{a}_n|V_n|\left(\overline{v}^2 - V_n^2\right)^{-1/2} \le \overline{a}_\tau. \tag{8}$$

Conversely, if all the listed inequalities are true with $\le \mapsto <$, the discussed controllability holds.

Now we assume that the conditions from Lemmas 1 and 2 hold with $>$ put in place of $\ge$ and that these $>$'s do not degrade to $\ge$ as $t \to \infty$. As a result, we arrive at the following.

Assumption 3.2. *There exist $\Delta_d, \Delta_v, \Delta_a, \Delta_a^\tau, \Delta_a^n > 0$ such that (3) and the first and second inequality in (5) remain true even if their r.h.s. are decreased by Δ_d, Δ_v, Δ_a, respectively. Also, the conditions from Lemma 2 remain true even if $\overline{a}_n \mapsto \overline{a}_n - \Delta_a^n$ and $\overline{a}_\tau \mapsto \overline{a}_\tau - \Delta_a^\tau$.*

This remains true if $\overline{v}, \overline{a}_n, \overline{a}_\tau$ and $\Delta_v, \Delta_a, \Delta_a^\tau, \Delta_a^n$ are slightly and coherently reduced. Let this be carried out. Then $\overline{v}$ is a feasible speed and $\overline{a}_n^2 + \overline{a}_\tau^2 \le \overline{a}^2 - \Delta_2$ for some $\Delta_2 > 0$.

The next requirement is usually fulfilled in the real world.

Assumption 3.3. *The configuration map $\Phi(\cdot)$, its first, second, and third derivatives, and the inverse to the Jacobian matrix $\Phi'_q(\cdot)$ are bounded on the domain of definition $O_* \times [0, \infty)$.*

Hence in (2), $d_\pm$ can be chosen so that the projection $\pi(\boldsymbol{r}, t)$ is unique and smoothly depends on $\boldsymbol{r}$ and t everywhere in Z_{op}. The following assumption addresses the visibility range of the robot.

Assumption 3.4. *There are $d_{\text{vis}}, \Delta_{\text{vis}} > 0$ such that if robots i, j are at a distance $\leq d_{\text{viz}}$ to Γ and the arc A of Γ between their projections has a length $\leq \Delta_{\text{vis}}$, robot i "sees" j and the arc A.*

Before the proposed control law is put in use, every robot should perform a simple maneuver. We omit elementary details of its implementation and merely state the targeted result of this maneuver.

Assumption 3.5. *At $t = 0$, the following claims hold. Every robot (1) has been accelerated to the maximal speed $\overline{v}$ and (2) has been driven far enough from the curve: there exists a straight line L such that $\Gamma(0)$ and the robot lie on the opposite sides of L and the distance d_L from the robot to L exceeds $(3\pi + 2)\overline{v}^2/\overline{a}$. Also, (3) during the first $3\pi\overline{v}/\overline{a}$ time units, the disc with a radius of $2\overline{v}^2/\overline{a}$ centered at the robot's initial location remains in Z_{op} and (4) the robots have been preliminarily driven so that they are far enough from one another: $\|\boldsymbol{r}_i(0) - \boldsymbol{r}_j(0)\| > 6\pi\overline{v}^2/\overline{a}$ whenever $i \neq j$.*

Implementability of (2) is due to (5) (in the enhanced form described in Assumption 3.2): by moving with a constant velocity and maximal speed, any robot can run arbitrarily far away from Γ. Different orientations of these velocities for different robots entail (4). The claim (3) in fact concerns the choice of $d_\pm$ in the definition of the operational zone.

4. Proposed communication-free hybrid nonlinear navigation law

A copy of this law individually operates on any robot. The law goes through two discrete modes:

$$\mathfrak{R}\,(\text{"reaching the curve"}) \xrightarrow{|d_i| \leq d_\downarrow} \mathfrak{T}\,(\text{"tracking the curve"}), \tag{9}$$

starting with $\mathfrak{R}$. Here $d_\downarrow > 0$ is a controller parameter. In $\mathfrak{R}$, the objective is to drive the robot to the curve Γ and to achieve the prescribed direction of motion over it, which is given by σ. In $\mathfrak{T}$, the task is to track the curve and to ensure and maintain an effective distribution of the robots over the curve.

Mode $\mathfrak{R}$. The control input $\boldsymbol{a}_i$ is generated by using a parameter $\mu > 0$ and map $\chi(\cdot) \in \mathbb{R}$:

$$\boldsymbol{a}_i = \sigma\overline{a} \cdot \textbf{sgn}\,\{\dot{d}_i + \mu\chi[d_i]\}\boldsymbol{u}_i^\perp, \quad \text{where} \quad \boldsymbol{u}_i = \boldsymbol{v}_i/v_i. \tag{10}$$

Numerical differentiation can be employed to assess the time derivative of the sensor readings $d_i(t)$; at the same time, any method is equally welcome.

Mode $\mathfrak{T}$ uses parameters $\overline{a}_n, \overline{a}_\tau, \varkappa_b, \Delta^s > 0$. Assumption 3.4 implies that if $|d_i| \leq d_{\text{viz}}$, robot i can compute (in its local frame) the projection $\boldsymbol{\varrho}_j$ and $s_{i\to j}$ for any robot j such that $|d_j| \leq d_{\text{viz}}$ and $|s_{i\to j}| \leq \Delta_{\text{viz}}$. Here $s_{i\to j}$ is the signed length of the arc of Γ with the end-points $\boldsymbol{\varrho}_i$ and $\boldsymbol{\varrho}_j$ counted in the direction of σ. We subject $d_\downarrow$ and Δ^s to

$$0 < d_\downarrow \leq d_{\text{viz}}, \qquad 0 < \Delta^s \leq \Delta_{\text{viz}}. \tag{11}$$

Definition 1. A *close neighbor* of robot i is robot $j \neq i$ such that $|d_j| < d_\downarrow$ and $|s_{i\to j}| < \Delta^s$. Such a neighbor is said to be *forward/backward* if $s_{i\to j} > 0/s_{i\to j} \leq 0$.

By Assumption 3.4 and (11), robot i can identify all its close neighbors and compute $s_i := \min_j s_{i\to j} > 0$, where $\min_j$ is over all close forward neighbors j of i if they exist; otherwise, $s_i := \Delta^s$.

https://doi.org/10.1017/S0263574721000667 Published online by Cambridge University Press

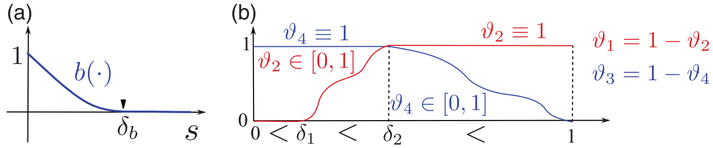

Figure 1. *Auxiliary functions defined by the parameters of the controller. (a) Function $b(\cdot)$. (b) Function $\vartheta(\cdot)$.*

Mode $\mathfrak{T}$. The control input $\boldsymbol{a}_i$ is generated by using a designer-chosen map $\Xi(\cdot):[0, \Delta^s] \to \mathbb{R}$:

$$\boldsymbol{a}_i = a_i^n \boldsymbol{e}_i - a_i^\tau \boldsymbol{e}_i^\perp, \quad \text{where} \quad \boldsymbol{e}_i = (\boldsymbol{\varrho}_i - \boldsymbol{r}_i)/\|\boldsymbol{\varrho}_i - \boldsymbol{r}_i\| \mathbf{sgn}\, d_i, \tag{12}$$

$$a_i^n := \bar{a}_n \cdot \mathbf{sgn}\,[\dot{d}_i + \mu\chi(d_i)], \quad a_i^\tau := -\bar{a}_\tau \cdot \mathbf{sgn}\,\Sigma_i(s_i, t) - b_i^\Sigma, \quad b_i^\Sigma := \varkappa_b \sum_j b\left(s_j\right), \tag{13}$$

$$\Sigma_i(s, t) := \vartheta_1\, \dot{\mathfrak{s}}_i + \vartheta_2 v_{i,\tau} - \sigma\left[\vartheta_3\sqrt{\left[\bar{v}^2 - v_{i,n}^2\right]_+} + \vartheta_4 \Xi(s)\right], \quad \vartheta_k = \vartheta_k(|d_i|/d_\downarrow). \tag{14}$$

Here $[b]_+ := \max\{b, 0\}$ and $b(\cdot)$, $\vartheta_k(\cdot)$ are designer-chosen smooth maps with the traits highlighted in Fig. 1, where $\delta_b > 0$, $0 < \delta_1 < \delta_2 < 1$. All forward close neighbors j of robot i are numbered in the order of the remoteness of $\boldsymbol{\varrho}_j$ from $\boldsymbol{\varrho}_i$ and, in the case of common $\boldsymbol{\varrho}_j$'s (if occur), in ascending order of d_j. If the robots do not collide with one another, these rules uniquely define an enumeration. In (13), the sum $\sum_j$ is from the least index to the first zero addend. (Any sum over the empty set is defined to be 0.) In the second formula from (13), the first addend is the main part of the control input, the second addend injects a "braking" correction to it. The idea behind the third formula in (13) is to set a "braking" effort b_i^Σ so that it exceeds the similar effort of any close robot j in front.

Access to the tangential $v_{i,\tau}$ and normal $v_{i,n}$ speeds of the robot may be, for example, due to evaluation of its own velocity $\boldsymbol{v}_i$ and the formulas $\boldsymbol{\tau} = -\boldsymbol{e}_i^\perp \mathbf{sgn}\, d_i, \boldsymbol{n} = \boldsymbol{\tau}^\perp$ (if $d_i \neq 0$) or direct estimation of the tangent $\boldsymbol{\tau}$ to Γ by using a local vision if $d_i \approx 0$. Computation of $\dot{\mathfrak{s}}_i := \left\langle \dot{\boldsymbol{\varrho}}_i; \boldsymbol{\tau}[\boldsymbol{\varrho}_i, t]\right\rangle$ may be based on, for example, access to the projection $\boldsymbol{\varrho}_i$ and numerical differentiation. If $\boldsymbol{\varrho}_i$ and $\boldsymbol{\tau}$ are evaluated in the local frame F_i of robot i and ^{l} signals about representation in F_i, then $\dot{\mathfrak{s}}_i = \left\langle \dot{\boldsymbol{\varrho}}_i^l; \boldsymbol{\tau}^l[\boldsymbol{\varrho}_i, t]\right\rangle + v_{i,\tau} - \varpi_i d_i$, where ϖ_i is the angular velocity of F_i. When close to Γ, we have, necessarily, $d_i \approx 0$, $\boldsymbol{\varrho}_i^l \approx 0$ and, often similarly, $\dot{\boldsymbol{\varrho}}_i^l \approx 0$. Then $\dot{\mathfrak{s}}_i \approx v_{i,\tau}$ and in (14), the sum of the first two addends $\approx v_{i,\tau}$.

For the above discontinuous control law, the closed-loop solutions are meant in the Filippov's sense [27]. Since this law generates bounded controls $\boldsymbol{a}_i$, the state $\boldsymbol{x} = \{(\boldsymbol{r}_i, \boldsymbol{v}_i)\}_{i=1}^N$ of the team obeys an ODE $\dot{\boldsymbol{x}} = f(\boldsymbol{x}, t)$, where $\|f(\boldsymbol{x}, t)\| \leq k(1 + \|\boldsymbol{x}\|)\ \forall \boldsymbol{x}, t$ with some $k > 0$. So given an initial state, the solution is defined for all $t \geq 0$ [27]. Its uniqueness is a more intricate issue. We do not come into its discussion and address all solutions, except for unviable ones. The latter are those that go on a repelling discontinuity manifold. For them, not only any state from this manifold gives rise to a solution going outside and away from the manifold but also almost all (all but a set of zero Lebesgue measure) arbitrarily small perturbations of the state cause "going outside and away". So the solutions that go on the manifold do not occur in practice due to their utmost finite-horizon instability.

5. Main results

The first result omits technical details on controller tuning in order to better highlight the key feature of the proposed control law: it does solve the mission, modulo being properly tuned.

Theorem 1. *Suppose that Assumptions 2.1–3.5 hold. Then the control law from Section 4 can be tuned so that the following claims are true:*

1. *All robots respect the speed and acceleration bounds: $v_i \leq \bar{v}$, $a_i \leq \bar{a}$ for all i and at any time;*
2. *Collisions among them do not occur and they remain in the operational zone (2);*

https://doi.org/10.1017/S0263574721000667 Published online by Cambridge University Press

3. *Any robot reaches the targeted curve: $d_i(t) \to 0$ as $t \to \infty$ for all i;*
4. *Eventually, the projections $\boldsymbol{\varrho}_i$ of different robots onto Γ are distinct, move over Γ in the desired direction $\sigma v_{i,\tau}(t) > 0$ and maintain a certain order: after a proper enumeration of the robots from 0 to $N-1$, the projection $\boldsymbol{\varrho}_{i\oplus 1}(t)$ (where $\oplus$ is addition modulo N) is the immediate predecessor of $\boldsymbol{\varrho}_i(t)$ in the direction given by σ;*
5. *Let the curve Γ be steady and let the visibility zone of any robot be nonempty under any even distribution of them over the curve: $\Delta_{vis} > P/N$. Here Δ_{vis} is taken from Assumption 3.4, P is the perimeter of Γ, and N is the number of the robots. Also, let $\Delta^s > P/N$ in (11). Then the robots asymptotically achieve an even distribution over the curve, that is, $s_{i\to i\oplus 1} \to P/N$ as $t \to \infty$, and sweep the curve with a speed that converges to $\Xi(P/N)$ as $t \to \infty$.*

Here 4 means nonclustering. Since P/N is the distance between two adjacent points of the even distribution over Γ, brutal violation $\Delta_{\text{vis}} < P/N$ of the condition $\Delta_{\text{vis}} > P/N$ from 5 means that when being close to the even distribution, the robots loose feedback from the inter-robot distances since they do not see one another. This makes the objective of their even distribution hardly feasible.

The remainder of the section discusses controller tuning.

Function $\boldsymbol{\chi(\cdot)}$ should be smooth and such that

$$z\chi(z) > 0\, \forall z \neq 0, \qquad \overline{\chi} := \sup_{z\in\mathbb{R}} |\chi(z)| < \infty, \quad \overline{\chi}' := \sup_{z\in\mathbb{R}} |\chi'(z\pm)| < \infty. \tag{15}$$

Examples are given by $\chi(z) = a\chi_*(z/b)$, where $a, b > 0$ and $\chi_*(z) = \arctan(z), \tanh(z), \frac{z}{\sqrt{1+z^2}}$.

Thresholds $d_\downarrow$ for (9) and $\boldsymbol{\Delta^s}$ for Definition 1 should be such that (11) is true and

$$d_\downarrow < d_L - (3\pi + 2)\overline{v}^2/\overline{a},\ \min\{|d_-|, d_+\}, \frac{\Delta_d \Delta_a^n}{2(\overline{\omega} + \overline{\varkappa}\,\overline{v})^2}, \frac{1}{\overline{\varkappa}}, \tag{16}$$

$$\left[\frac{(\overline{\omega} + \overline{\varkappa v})\overline{\varkappa}'(\overline{v} + \overline{\omega} d_\downarrow)d_\downarrow}{(1-\overline{\varkappa} d_\downarrow)^3} + \frac{\overline{\epsilon}}{1-\overline{\varkappa} d_\downarrow} + \frac{(\overline{\wp} + \overline{\omega}'_{\boldsymbol{\varrho}} + \overline{v\varkappa}'_{\boldsymbol{\varrho}})(\overline{v} + \overline{\omega} d_\downarrow)}{(1-\overline{\varkappa} d_\downarrow)^2}\right]\delta_2 d_\downarrow < \frac{\Delta_a^\tau}{6}, \tag{17}$$

$$\frac{\overline{\omega} + \overline{\varkappa v}}{1-\overline{\varkappa} d_\downarrow}\delta_2 d_\downarrow < \frac{1}{2}\sqrt{\overline{v}\Delta_v - \Delta_v^2/4}, \ \frac{\overline{\varkappa} d_\downarrow}{1-\overline{\varkappa} d_\downarrow}\left\{\overline{a} + 2\frac{(\overline{\omega} + \overline{\varkappa v})\overline{v}}{1-\overline{\varkappa} d_\downarrow}\right\}\left[1 + \frac{\overline{v}}{\sqrt{\overline{v}\Delta_v - \Delta_v^2/4}}\right] < \frac{\Delta_a^\tau}{6}. \tag{18}$$

Here d_L and $d_\pm$ is taken from (2) in Assumption 3.5 and (2), respectively, $\Delta_d, \Delta_v, \Delta_a^\tau, \Delta_a^n > 0$ are the constants from Assumption 3.2, and the following constant and finite bounds are also used:

$$|q(\boldsymbol{\varrho}, t)| \leq \overline{q} \quad \forall \boldsymbol{\varrho} \in \Gamma(t), \forall t \text{for } q = \varkappa, \omega, \varkappa'_{\boldsymbol{\varrho}}, \omega'_{\boldsymbol{\varrho}}, \epsilon, \wp; \quad 0 < \underline{p} \leq \textbf{Perim}[\Gamma(t)] \leq \overline{p}\, \forall t. \tag{19}$$

Here $_{\boldsymbol{\varrho}}$ refers to the derivative in the tangential direction, and **Perim**$[\Gamma]$ is the perimeter of Γ. In (19), finite bounds do exist thanks to Assumption 3.3. All the inequalities in (16)–(18) are met by taking $d_\downarrow$ small enough since their r.h.s.'s are positive by (2) in Assumption 3.5.

Function $\boldsymbol{\Xi(s)}$ of $s \in [0, \Delta^s]$ is smooth and such that

$$\Xi(0) \geq 0, \quad \underline{\Xi}' := \min_{s\in[0,\Delta^s]} \Xi'(s) > 0, \quad \overline{\Xi} := \max_{s\in[0,\Delta^s]} \Xi(s) < \frac{1}{2}\sqrt{\overline{v}\Delta_v - \Delta_v^2/4}, \tag{20}$$

$$\overline{\Xi}' := \max_{s\in[0,\Delta^s]} \Xi'(s) < \frac{\Delta_a^\tau(1-\overline{\varkappa} d_\downarrow)}{6[2(\overline{v} + \overline{\omega} d_\downarrow) + (1-\overline{\varkappa} d_\downarrow)\overline{p}\,\overline{\varkappa}\,\overline{v}]}. \tag{21}$$

These are met by, for example, any linear ascending function with sufficiently small slope and range.

https://doi.org/10.1017/S0263574721000667 Published online by Cambridge University Press

Parameter $\boldsymbol{\mu}$ is chosen by using $\overline{\chi}$ from (15) and so small that the following hold:

$$2\mu\overline{\chi} \leq \Delta_v, \quad \frac{\overline{a}\sqrt{2\mu\overline{\chi}}}{\sqrt{\overline{v}}} + 2\frac{\overline{\varkappa}\,\overline{v}\,\overline{\chi}\mu + \overline{\omega}\sqrt{2\overline{v}\,\overline{\chi}\mu}}{\Delta_d} + \mu^2\overline{\chi}\,\overline{\chi}' < \Delta_a,$$

$$2\overline{v}\mu\overline{\chi}\left[\left(1+\frac{\overline{v}\mu\overline{\chi}}{\Delta_v^2}\right)\overline{\varkappa} + \frac{\overline{\omega}}{\Delta_v}\right] + \mu^2\overline{\chi}\,\overline{\chi}' < \frac{\Delta_a^n}{2}, \tag{22}$$

$$\frac{(\overline{v}+\overline{\Xi})\overline{\vartheta}_3'}{d_\downarrow} + \frac{\overline{v}^3[\overline{a}_n + (\overline{\omega}+\overline{\varkappa v})\overline{v}]}{(\overline{v}\Delta_v - \Delta_v^2/4)^{3/2}} + \frac{(\overline{\vartheta}_1'+2)(\overline{\omega}+\overline{\varkappa v})}{(1-\overline{\varkappa}d_\downarrow)^2}$$
$$+\left[\overline{\varkappa} + \frac{(\overline{\omega}+2\overline{\varkappa v})}{\sqrt{\overline{v}\Delta_v - \Delta_v^2/4}}\right]\frac{\overline{v}^2}{\sqrt{\overline{v}\Delta_v - \Delta_v^2/4}} < \frac{\Delta_a^\tau}{6\mu\overline{\chi}}. \tag{23}$$

Here $\overline{\vartheta}_k$ is an upper bound on the absolute value of the derivative of the function $\vartheta_k(\cdot)$ from Fig. 1(b).

Parameter $\boldsymbol{\delta_b}$ from Fig. 1(a) is chosen with invoking $\underline{p}$ from (19) and so small that

$$\delta_b < \Delta^s/N, \underline{p}/N. \tag{24}$$

Parameter $\boldsymbol{\varkappa_b}$ from (13) is chosen with using Δ_2 (introduced after Assumption 3.2) and so small that

$$0 < \varkappa_b < \Delta_a^\tau/(6N), \quad 2\overline{a}N\varkappa_b + N^2\varkappa_b^2 < \Delta_2. \tag{25}$$

Theorem 2. *Let the assumptions of Theorem 1 hold and the parameters of the control law be chosen subject to the above recommendations. Then the claims 1–4 of Theorem 1 are true. If the additional assumptions of 5 from Theorem 1 hold and $\Delta^s := \Delta_{vis}$, the claim 5 is true as well.*

The above recommendations on the choice of the controller parameters can be used as general guidelines for experimentally tuning the controller. If estimates of the involved quantities (like $\overline{\varkappa}, \overline{p}$, etc.) are available, they can be used for analytically tuning.

6. Computer simulation tests

The numerical values of the basic parameters used in the tests are as follows: $\overline{a} = 3.0\ \mathrm{m/s^2}$, $\overline{v} = 5.0\ \mathrm{m/s}$, $\Delta_{\mathrm{viz}} = 100.0\ \mathrm{m}$, $d_{\mathrm{viz}} = 2.0\ \mathrm{m}$, $\mu = 0.01\ \mathrm{m/s}$, $\chi(d) = 300 \arctan \frac{d}{20}$, $\overline{a}_n = 2.0\ \mathrm{m/s^2}$, $\overline{a}_\tau = \sqrt{5}\ \mathrm{m/s^2}$, $d_\downarrow = 1.5\ \mathrm{m}$, $\Delta^s = 20\pi\ \mathrm{m}$, $\Xi(s) = 4\ \mathrm{s}/\Delta^s$, $\delta_b = 0.2\ \mathrm{m}$, $\varkappa_b = 0.002\ \mathrm{m/s^2}$, the control update period $\tau = 0.05\ \mathrm{s}$; in Fig. 1, $\delta_1 = 1/4$, $\delta_2 = 1/2$ and all functions are linear on the intervals where they are not constant. The distance measurements were corrupted by noises evenly distributed over $[-0.005\ \mathrm{m}, 0.005\ \mathrm{m}]$. (This corresponds to reaching distances of hundreds of meters with accuracies of several centimeters and is even worse than for many modern distance sensors.) The two-point Newton quotient was used to estimate time-derivatives. Multimedia of the extended versions of all tests are available at https://drive.google.com/drive/folders/18BN633CaCsu_I_5ERBZZqG0euRbs9_NN?usp=sharing

In Figs. 2–5, the robots are depicted as small colored discs, a short segment attached to the disc shows the orientation of the velocity vector. The targeted curve Γ is depicted in black. In the last picture of any figure, every colored graph visualizes the distance (over the curve Γ) from the robot with the same color to its immediate predecessor. (More precisely, the distance between their projections onto the curve is meant.)

In Fig. 2, Γ is a circle, and an intricacy is due to its motion along the "vertical" axis and periodic pulsation of its radius. Figure 2(a) displays the initial deployment of six robots $N = 6$. In Fig. 2(b), four of them reach Γ and turn on mode $\mathfrak{T}$, two robots are still in $\mathfrak{R}$, and only on approach of Γ. Figure 2(c) shows that ≈ 14.0 s later, all robots are in mode $\mathfrak{T}$ and reach a very close proximity of Γ; in fact, they remain there afterward. Meanwhile, the blue and brown robots form somewhat like a cluster. In Fig. 2(d) (that is, ≈ 30.0 s later), this cluster is broken, and the robots achieve a cluster-free and nearly homogeneous distribution over Γ. Afterward, these traits were maintained, and the robots did not overtake one another;

https://doi.org/10.1017/S0263574721000667 Published online by Cambridge University Press

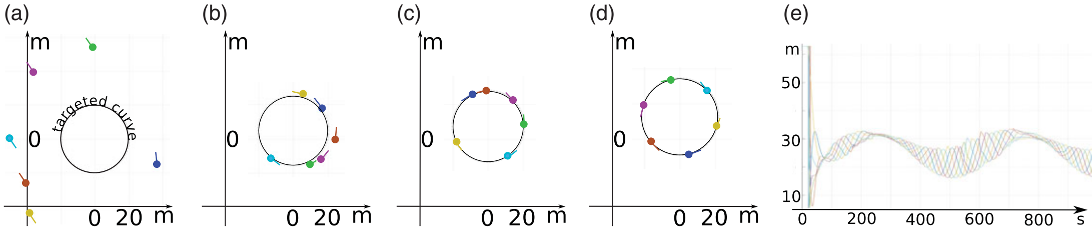

Figure 2. *Tracking and self-distribution over a moving and pulsating circle. (a)* $t = 0.0$ *s. (b)* $t = 26.0$ *s. (c)* $t = 40.0$ *s. (d)* $t = 70.0$ *s. (e) Inter-robot distances.*

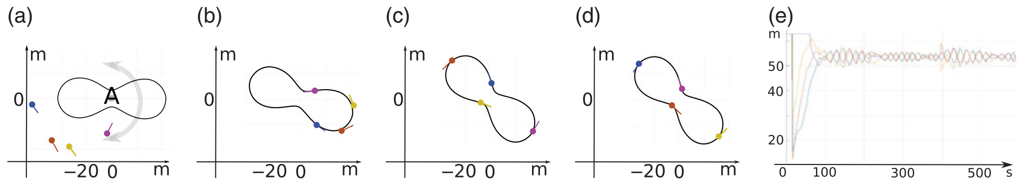

Figure 3. *Tracking a swinging rigid curve. (a)* $t = 0.0$ *s. (b)* $t = 26.0$ *s. (c)* $t = 62.0$ *s. (d)* $t = 77.0$ *s. (e) Inter-robot distances.*

they also never collided. Meanwhile, Fig. 2(e) shows that the even distribution is not achieved. This effect is expected in the case of a stretching/contracting curve and is due to the fact that control is by means of the second derivative (acceleration), and there is no feedback from the first derivative of the discussed regulated output, which is the length of the dynamic arc (of Γ) between the robot and its predecessor. Indeed, the control law (12)–(14) implements a feedback from the velocities of the end-points of this arc, but its length is also dependent on the curve's own stretching/contracting. In (12)–(14), the lack of feedback from the velocities of the curve is inspired by the fact that reliable online measurement or estimation of velocities of outer objects, especially the rates of stretching/shortening, still represents a real challenge in practical setting; in this regard, the purpose of this paper is to set a theoretical benchmark by unveiling the horizon achievable without assessing these velocities. As can be seen in Fig. 2(d), (e), the deviation from the even distribution is not substantial, and the control law eventually ensures more or less even and surely cluster-free coverage of the curve. In Fig. 2(e), the disparity in the inter-robot distances is correlated with the rates of change in the curve length: the lesser the rate, the lesser the disparity.

In Fig. 3, four robots $N = 4$ should reach and then trace a rigid curve, which periodically swings clockwise/counterclockwise about the steady pivot A in the geometrical center of the curve. The initial deployment is shown in Fig. 3(a). As can be seen in Fig. 3(b), the robots promptly reach Γ and turn on mode $\mathfrak{T}$, though leave a half of Γ unattended. Not later than in Fig. 3(c), the distribution of the robots becomes much more uniform and there remains no unattended half-curve. Since Fig. 3(d), the distribution is nearly even, as is illustrated by Fig. 3(d), (e); in fact, the mean deviation of the inter-robot distance from the ideal value is $\approx \pm 5\%$ In this experiment, the initial locations of the robots are intentionally chosen outside any zone of the form (2) for which Assumption 3.1 holds and guarantees the uniqueness of the projection onto Γ so that Assumption 3.5 is violated. Meanwhile, no problems with the convergence of the control law are revealed in this case.

Figure 4 addresses a scenario with substantial alterations of the curve's shape. In Fig. 4(b), all four robots reach a close proximity of the curve and turn on mode $\mathfrak{T}$; meanwhile, their distribution over the curve is far from being even and approximately a half-curve is unattended. As is illustrated in Fig. 4(e), (d), not later than ≈ 50 s later they achieve a nearly homogeneous self-distribution and maintain it afterward while constantly sweeping the entirety of the pulsating and reshaping curve. In this experiment, the exactness of distribution is even better than in Fig. 3, which may be associated with the fact that under

https://doi.org/10.1017/S0263574721000667 Published online by Cambridge University Press

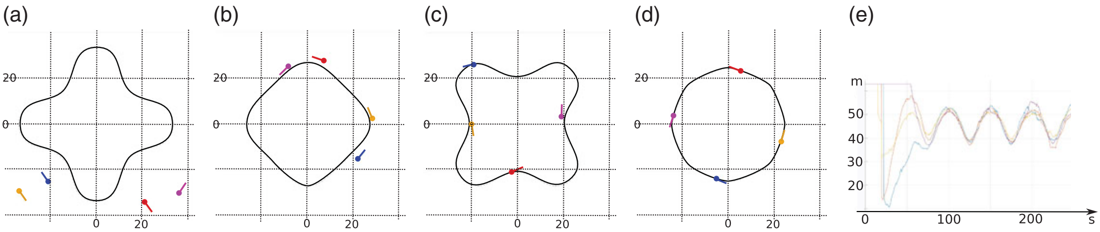

Figure 4. *Reaching a pulsating and deforming curve, with subsequent even distribution over it. (a) $t = 0.0$ s. (b) $t = 21.0$ s. (c) $t = 51.0$ s. (d) $t = 75.0$ s. (e) Inter-robot distances.*

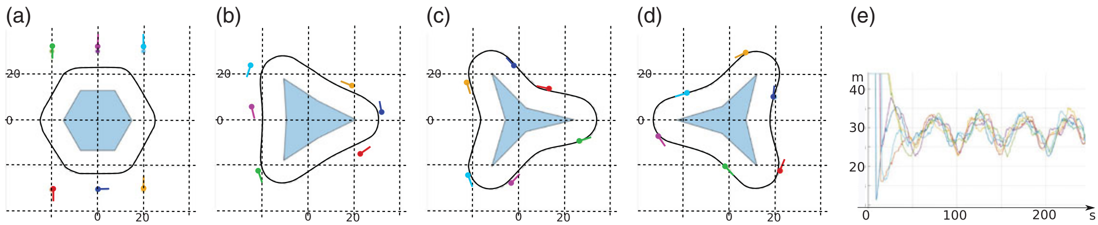

Figure 5. *Circumnavigation and surrounding of a rapidly reconfiguring extended body. (a) $t = 0.0$ s. (b) $t = 10.0$ s. (c) $t = 24.0$ s. (d) $t = 68.0$ s. (e) Inter-robot distances.*

any even deployment of four robots on the curve, the arcs from any robot to its immediate predecessor are congruent to one another due to the curve's symmetry.

With respect to Figs. 2–4, we do not discuss the origin and genesis of the targeted curve. For the scenario in Fig. 5, this is the locus of points at a given distance d_0 from a reconfigurable extended body depicted in blue. An extra challenge stems from the fact that the reconfiguration process is fairly fast, for example, for ≈ 1.0 min, the body goes through the sequence of highly different shapes shown in Fig. 5(a)–(d). Despite this, the proposed control law not only drives all robots to the targeted equidistant curve but also ensures their clusterless effective distribution over this curve, which differs from the even one by only $\approx 8\%$ in relative terms. Anyway, the body becomes promptly surrounded from all sides with a mobile barrier perpetually sweeping the equidistant curve, as is required.

The controller (13) is fed by the length s of the Γ-arc between the projections of the robots onto Γ. This gives rise to the trend toward the uniformity of the robots' distribution over Γ, which trend is attested by the above figures. However, determining the arc length may be computationally expensive and inaccurate for highly contorted curves. This is among the incentives not to feed the controller by the time derivative of the measured arc length since by its own right, numerical differentiation carries a potential for the error aggravation. The next step might consist in modification of the control law via defining s as the straight line distance between the projections or even the robots themselves. We leave study of this modification as a topic of further research.

7. Conclusions

The paper proposed a distributed control law that autonomously drives speed- and acceleration-limited robots to an unpredictably moving and deforming Jordan curve and ensures subsequently tracking this curve in a common prespecified direction, along with cluster-free distribution of the robots over this curve; this distribution is proven to be even if the curve is steady. The global convergence of the control law is rigorously justified and confirmed via computer simulation tests.

Acknowledgments. This research was supported by the Russian Science Foundation under the grant 19-19-00403.

Conflicts of Interest. The authors declare none.

References

[1] K. Oh, M. Park and H. Ahn, "A survey of multi-agent formation control," *Automatica* **53**, 424–440 (2015).
[2] W. Ren and Y. Cao, *Distributed Coordination of Multi-agent Networks: Emergent Problems, Models, and Issues* (Springer-Verlag, London, 2010)
[3] N. Ceccarelli, M. DiMarco, A. Garulli and A. Giannitrapani, "Collective circular motion of multi-vehicle systems," *Automatica* **44**(12), 3025–3035 (2008).
[4] J. Guo, G. Yan and Zh. Lin, "Local control strategy for moving-target-enclosing under dynamically changing network topology," *Syst. Control Lett.* **59**(10), 654–661 (2010).
[5] H. Kawakami and T. Namerikawa, "Cooperative Target-Capturing Strategy for Multi-Vehicle Systems with Dynamic Network Topology," *Proceedings of the 2009 ACC* (2009) pp. 635–640.
[6] T. Kim, Sh. Harab and Y. Hori, "Cooperative control of multi-agent dynamical systems in target-enclosing operations using cyclic pursuit strategy," *Int. J. Control* **83**(10), 2040–2052 (2010).
[7] T. Kim and T. Sugie, "Cooperative control for target-capturing task based on a cyclic pursuit strategy," *Automatica* **43**(8), 1426–1431 (2007).
[8] Y. Kobayashi and Sh. Hosoe, "Cooperative enclosing and grasping of an object by decentralized mobile robots using local observation," *Int. J. Soc. Rob.* **4**(1), 19–32 (2012).
[9] M. Kothari, R. Sharma, I. Postlethwaite, R. Beard and D. Pack, "Cooperative target-capturing with incomplete target information," *Int. J. Intell. Rob. Syst.* **72**(3–4), 373–384 (2013).
[10] Y. Lan, G. Yan, and Zh. Lin, "Distributed control of cooperative target enclosing based on reachability and invariance analysis," *Syst. Control Lett.* **59**(7), 381–389 (2010).
[11] J. A. Marshall, M. E. Broucke and B. A. Francis, "Pursuit formations of unicycles," *Automatica* **42**(1), 3–12 (2006).
[12] I. Shames, B. Fidan and B. D. O. Anderson, "Close target reconnaissance with guaranteed collision avoidance," *Int. J. Robust Nonlinear Control* **21**(16), 1823–1840 (2011).
[13] A. Sinha and D. Ghose, "Generalization of nonlinear cyclic pursuit," *Automatica* **43**(11), 1954–1960 (2007).
[14] K. Tsumura, S. Hara, K. Sakurai and T. H. Kim, "Performance competition in cooperative capturing by multi-agent systems," *SICE J. Control Meas. Syst. Integr.* **4**(3), 221–229 (2011).
[15] H. Yamaguchi, "A distributed motion coordination strategy for multiple nonholonomic mobile robots in cooperative hunting operations," *Rob. Auto. Syst.* **43**(4), 257–282 (2003).
[16] A. Zakhar'eva, A. S. Matveev, M. C. Hoy and A. V. Savkin, "A strategy for target capturing with collision avoidance for non-holonomic robots with sector vision and range-only measurements," *Robotica* **33**(2), 385–412 (2015).
[17] A. V. Savkin, T. M. Cheng, Z. Xi, F. Javed, A. S. Matveev and H. Nguyen, *Decentralized Coverage Control Problems for Mobile Robotic Sensor and Actuator Networks* (Wiley and IEEE Press, Hoboken, NJ, 2015)
[18] K. Sato and N. Maeda, "Target-Enclosing Strategies for Multi-Agent Using Adaptive Control Strategy," *Proceedings of the 2010 IEEE International Conference on Control Applications* (2010) pp. 1761–1766.
[19] A. S. Matveev and K. S. Ovchinnikov, "Circumnavigation of a speedy unpredictable target by a group of speed- and acceleration-limited robots," *Int. J. Robust Nonlinear Control* **29**(4), 1063–1087 (2019).
[20] M. Deghat, L. Xia, B. D. O. Anderson and Y. Hong, "Multi-target localization and circumnavigation by a single agent using bearing measurements," *Int. J. Robust Nonlinear Control* **25**(14), 2362–2374 (2015).
[21] A. S. Matveev, A. A. Semakova and A. V. Savkin, "Range-only based circumnavigation of a group of moving targets by a non-holonomic mobile robot," *Automatica* **65**, 76–89 (2016).
[22] A. S. Matveev, A. A. Semakova and A. V. Savkin, "Tight circumnavigation of multiple moving targets based on a new method of tracking environmental boundaries," *Automatica* **79**, 52–60 (2017).
[23] K. S. Ovchinnikov, A. A. Semakova and A. S. Matveev, "Cooperative surveillance of unknown environmental boundaries by multiple nonholonomic robots," *Rob. Auto. Syst.* **72**, 164–180 (2015).
[24] A. S. Matveev, C. Wang and A. V Savkin, "Real-time navigation of mobile robots in problems of border patrolling and avoiding collisions with moving and deforming obstacles," *Rob. Auto. Syst.* **60**(6), 769–788 (2012).
[25] J. A. M. Spencer, *Continuum Mechanics* (Dover Publications, NY, 2004)
[26] A. S. Matveev, H. Teimoori and A. V. Savkin, "A method for guidance and control of an autonomous vehicle in problems of border patrolling and obstacle avoidance," *Automatica* **47**(3), 515–524 (2011).
[27] A. F. Filippov, *Differential Equations with Discontinuous Righthand Sides* (Kluwer Academic Publishers, Dordrecht, the Netherlands, 1988).
[28] H. Altenbach and A. Öchsner, (eds.), *Encyclopedia of Continuum Mechanics* (Springer, Berlin, 2020)

[29] A. S. Matveev and V. V. Magerkin, "Robotic following of flexible extended objects: Relevant technical facts on the kinematics of a moving continuum," ArXiv 2012.13240 (2020).
[30] J. M. Danskin, "The theory of min-max, with applications," *SIAM J. Appl. Math.* **14**(4), 641–644 (1966).
[31] P. Hartman, *Ordinary Differential Equations*, 2nd edn. (Birkhäuzer, Boston, 1982).

A. Proofs: Preliminaries

Owing to the nature of the control objective, kinematical, and other characteristics of the moving and deforming curve play a key role in mathematically rigorous justification of the algorithm. From a general perspective, this curve is a dynamic continuum. Up to now, such continua were mostly studies within the framework of the continuum mechanics [25, 28]. However, this discipline is mostly focused on the mechanical behavior of materials modeled as a continuous mass, is not much concerned with navigation of robots relative to continua, and so does not offer many formulas needed in research on robotics. This gap is partly filled in ref. [29]. For convenience of the reader, this section replicates some basic formulas from ref. [29], their justification is presented in ref. [29].

The arguments of a map may be dropped if they are clear from the context. We use the following notations:

- $\boldsymbol{\varrho}_\Gamma(\theta|t,\boldsymbol{\varrho})$, location of the point $\boldsymbol{\varrho} \in \Gamma(t)$ at time θ;
- $L_t(\boldsymbol{\varrho}' \to \boldsymbol{\varrho}'')$, signed length of the arc of $\Gamma(t)$ from $\boldsymbol{\varrho}' \in \Gamma(t)$ to $\boldsymbol{\varrho}'' \in \Gamma(t)$, countered counterclockwise;
- $\varsigma(\varrho,t) := \lim_{\theta\to t,\delta\to 0} \frac{L_\theta[\boldsymbol{\varrho}_\Gamma(\theta|t,\boldsymbol{\varrho})\to\boldsymbol{\varrho}_\Gamma(\theta|t,\boldsymbol{\varrho}_\delta)]-\delta}{(\theta-t)\delta}$, rate of stretch of Γ at $\boldsymbol{\varrho} \in \Gamma(t)$; here $\boldsymbol{\varrho}_\delta \in \Gamma(t)$ is determined by $L_t[\boldsymbol{\varrho} \to \boldsymbol{\varrho}_\delta] = \delta$.

The first lemma unites Theorem 2.2 and the first statement of Theorem 2.4 from ref. [29].

Lemma A1. *The following relations hold for any robot i, at any time t, and for any point $\boldsymbol{\varrho} \in \Gamma(t)$:*

$$\boldsymbol{\varrho}_i(t+dt) - \pi[\boldsymbol{\varrho}_i, t+dt] = \dot{\mathfrak{s}}_i \boldsymbol{\tau} dt + o(dt),$$

$$\langle \dot{\boldsymbol{\varrho}}_i; \boldsymbol{n}\rangle = V_n, \quad \frac{d\boldsymbol{\tau}[\boldsymbol{\varrho}_i(t),t]}{dt} = (\omega + \varkappa\,\dot{\mathfrak{s}}_i)\boldsymbol{n}, \quad \frac{d\boldsymbol{n}[\boldsymbol{\varrho}_i(t),t]}{dt} = -(\omega+\varkappa\,\dot{\mathfrak{s}}_i)\boldsymbol{\tau}, \tag{A1}$$

$$\pi(\boldsymbol{\varrho},\theta) = \boldsymbol{\varrho} + V_n(\boldsymbol{\varrho},t)\boldsymbol{n}(\boldsymbol{\varrho},t)(\theta-t) + o(\theta-t), \tag{A2}$$

$$\varsigma(\boldsymbol{\varrho},t) = \langle \boldsymbol{\tau}(\boldsymbol{\varrho},t); V_{\boldsymbol{\varrho}}'(\boldsymbol{\varrho},t)\rangle, \qquad \omega(\varrho,t) = \langle \boldsymbol{n}(\boldsymbol{\varrho},t); V_{\boldsymbol{\varrho}}'(\boldsymbol{\varrho},t)\rangle - \varkappa(\boldsymbol{\varrho},t)V_\tau(\boldsymbol{\varrho},t); \tag{A3}$$

$$\dot{V}_n := \frac{dV_n[\boldsymbol{\varrho}_i(t),t]}{dt} = \dot{\mathfrak{s}}_i\omega - \varkappa V_\tau^2 - 2\omega V_\tau + A_n, \quad \left\| \frac{\partial \pi}{\partial \boldsymbol{\varrho}}(\boldsymbol{\varrho}, t+dt)\right\| - 1 = -\varkappa(\boldsymbol{\varrho},t)V_n(\boldsymbol{\varrho},t)dt + o(dt), \tag{A4}$$

$$\varkappa[\pi(\boldsymbol{\varrho},t+dt),t+dt] = \varkappa(\boldsymbol{\varrho},t) + (\omega_\rho' + \varkappa^2 V_n)dt + o(dt), \tag{A5}$$

$$V_n[\pi(\boldsymbol{\varrho},t+dt),t+dt] = V_n[\boldsymbol{\varrho},t] - (2\omega V_\tau - A_n + \varkappa V_\tau^2)dt + o(dt), \tag{A6}$$

$$\sigma\dot{s}_{i\to j}(t) = \dot{\mathfrak{s}}_j(t) - \dot{\mathfrak{s}}_i(t) - \oint_{\boldsymbol{\varrho}_i(t)}^{\boldsymbol{\varrho}_j(t)} \varkappa(\boldsymbol{\varrho},t)V_n(\boldsymbol{\varrho},t)ds, \tag{A7}$$

where s is the arc length and $\oint \dots ds$ is the integral along $\Gamma(t)$.

The next lemma encompasses Theorem 2.3 and the second statement of Theorem 2.4 from ref. [29].

Lemma A2. *For $v_{i,\tau} = \langle \boldsymbol{v}_i; \boldsymbol{\tau}\rangle$, $v_{i,n} = \langle \boldsymbol{v}_i; \boldsymbol{n}\rangle$ and any robot i, the following relations hold:*

$$\dot{d}_i = V_n - v_{i,n}, \qquad \dot{\mathfrak{s}}_i = \frac{v_{i,\tau} - \omega d_i}{1+\varkappa d_i} = v_{i,\tau} - \frac{\omega + \varkappa v_{i,\tau}}{1+\varkappa d_i}d_i, \qquad \omega + \varkappa\,\dot{\mathfrak{s}}_i = \frac{\omega+\varkappa v_{i,\tau}}{1+\varkappa d_i}, \tag{A8}$$

$$\boldsymbol{v}_i = [V_n - \dot{d}_i]\boldsymbol{n} + [\,\dot{\mathfrak{s}}_i(1+\varkappa d_i) + \omega d_i]\boldsymbol{\tau}, \ddot{d}_i = \frac{\varkappa v_{i,\tau}^2 + 2v_{i,\tau}\omega - \omega^2 d_i}{1+\varkappa d_i} - \varkappa V_\tau^2 - 2\omega V_\tau + A_n - a_{i,n}, \tag{A9}$$

https://doi.org/10.1017/S0263574721000667 Published online by Cambridge University Press

$$\dot{v}_{i,\tau} = a_{i,\tau} + \frac{\omega + \varkappa v_{i,\tau}}{1 + \varkappa d_i} v_{i,n} = a_{i,\tau} + (\omega + \varkappa \dot{\mathfrak{s}}_i) v_{i,n}; \dot{v}_{i,n} = a_{i,n} - \frac{\omega + \varkappa v_{i,\tau}}{1 + \varkappa d_i} v_{i,\tau} = a_{i,n} - (\omega + \varkappa \dot{\mathfrak{s}}_i) v_{i,\tau}. \quad \text{(A10)}$$

$$\sigma \ddot{s}_{i \to j}(t) = a_{j,\tau} - a_{i,\tau} + \lambda_j - \lambda_i - \oint_{\varrho_i}^{\varrho_j} \mathfrak{A}\, ds, \quad \text{where } \mathfrak{A} := \omega'_\rho V_n - 2\omega\varkappa V_\tau + \varkappa A_n - \varkappa^2 V_\tau^2, \quad \text{(A11)}$$

$$\lambda_k := \omega V_n - \frac{2\dot{d}_k[\omega + \varkappa \dot{\mathfrak{s}}_k] + [\dot{\omega} + \dot{\varkappa} \dot{\mathfrak{s}}_k + \varkappa a_{k,\tau} + (\dot{\mathfrak{s}}_k \varkappa + \omega)\varkappa V_n] d_k}{1 + \varkappa d_k},$$
$$\dot{\omega} = \omega'_\varrho \dot{\mathfrak{s}}_i + \epsilon, \ \dot{\varkappa} = \varkappa'_\varrho \dot{\mathfrak{s}}_i + \wp. \quad \text{(A12)}$$

B. Proofs of the lemmas from section 3

Proof of Lemma 1: By (A9) and (A8), $\dot{d}_i = 0 \Rightarrow \boldsymbol{v}_i = V_n \boldsymbol{n} + v_{i,\tau} \boldsymbol{\tau}$. Since $\|\boldsymbol{v}_i\| = \overline{v}$, the first inequality in (5) holds with $\leq \mapsto <$ and $v_{i,\tau} = \mathbf{sgn}\, v_{i,\tau} \sqrt{\overline{v}^2 - V_n^2}$. By (4) and (A9), $\ddot{d}_i = \mathcal{A} - a_{i,n}$, where $\mathcal{A} := \gamma_{\mathbf{sgn}\, v_{i,\tau}}(d_i, \boldsymbol{\varrho}_i, t, V_n)$. Meanwhile, $\|\boldsymbol{a}_i\| \leq \overline{a}$ and $v \equiv \overline{v} \Rightarrow \langle \boldsymbol{a}_i; \boldsymbol{v}_i \rangle \equiv 0$. So we see that $a_{i,n}$ can be manipulated only within $[-\alpha, \alpha]$, where $\alpha = |v_\tau| \overline{a}/\overline{v} = \overline{a}\sqrt{1 - V_n^2/\overline{v}^2}$. Hence, the capacity to freely manipulate the sign of $\ddot{d}_i$ holds if and only if $|\mathcal{A}| < \alpha$. This entails (5). □

Proof of Lemma 2: Being on Γ means that $d_i = 0, \dot{d}_i = 0$. So by (A9), $v_{i,n} = V_n$, $|V_n| \leq v_i$, $v_{i,\tau} = \mathbf{sgn}\, v_{i,\tau} \sqrt{v_i^2 - V_n^2}$, and

$$\dot{g}_{\pm,i} \overset{(6)}{=} \dot{v}_{i,\tau} \mp \frac{\dot{v}_{i,n} v_{i,n}}{\sqrt{\overline{v}^2 - v_{i,n}^2}} \overset{(A10)}{=} a_{i,\tau} + (\omega + \varkappa v_{i,\tau}) V_n \mp \frac{V_n}{\sqrt{\overline{v}^2 - V_n^2}} \left[a_{i,n} - (\omega + \varkappa v_{i,\tau}) v_{i,\tau} \right].$$

By (A9), the capacity described in (i) of Definition 1 holds if and only if for all $\zeta \in \left[0, \sqrt{\overline{v}^2 - V_n^2}\right)$,

$$\left| \varkappa \zeta^2 \pm 2\omega\zeta - \varkappa V_\tau^2 - 2\omega V_\tau + A_n \right| < \overline{a}_n, (|\omega| + |\varkappa|\zeta)|V_n| + \frac{|V_n|}{\sqrt{\overline{v}^2 - V_n^2}} [\overline{a}_n + (|\omega| + |\varkappa|\zeta)\zeta] < \overline{a}_\tau. \quad \text{(B13)}$$

The first relation holds on the considered interval of ζ if and only if it holds (with $< \mapsto \leq$) at its right end and also at the vertex $\zeta_v = \mp\omega/\varkappa$ of the parabola if ζ_v conforms to the interval $|\omega| < |\varkappa|\sqrt{\overline{v}^2 - V_n^2}$. Here the first and second condition are identical to (5) with $\overline{a} := \overline{a}_n, d = 0, < \mapsto \leq$ and to (7), respectively. Since the l.h.s. of the second relation in (B13) increases with $\zeta \geq 0$, this relation holds if and only if its l.h.s. does not exceed $\overline{a}_\tau$ for $\zeta = \sqrt{\overline{v}^2 - V_n^2}$. Thus, we arrive at (8). □

C. Proofs of theorems 1 and 2: behavior in mode $\mathfrak{R}$

In this section, we adopt the assumptions of Theorem 2 and, except for Lemma C3, focus on a particular robot and so drop its index i. We also put $S := \dot{d} + \mu\chi(d)$, and consider the surface $\mathcal{S}$ in the space of phase variables $\boldsymbol{r}, \boldsymbol{v}, t$ given by $S = 0$ and $(\boldsymbol{r}, t) \in Z_{\text{op}}$.

Lemma C1. *(1) The tangential speed v_τ is nonzero on the part $\mathcal{S}_{\overline{v}}$ of $\mathcal{S}$ where $v = \overline{v}$. (2). In mode $\mathfrak{R}$, the surface $\mathcal{S}$ is sliding (two-side repelling) at any point of $\mathcal{S}_{\overline{v}}$ where $\sigma v_\tau > 0$ (respectively, $\sigma v_\tau < 0$).*

Proof . We will systematically use the following conditions for the sliding/repelling mode [27]:

$$\lim_{S \neq 0, S \to 0} \dot{S}\, \mathbf{sgn}\, S < 0 \Rightarrow \text{sliding}, \qquad \lim_{S \neq 0, S \to 0} \dot{S}\, \mathbf{sgn}\, S > 0 \Rightarrow \text{repelling}. \quad \text{(C1)}$$

https://doi.org/10.1017/S0263574721000667 Published online by Cambridge University Press

By taking into account Assumption 3.2, (15), and (A9), we see that whenever $v = \overline{v}$,

$$S = 0 \Rightarrow |v_n - V_n| = |\langle \boldsymbol{v}; n\rangle - V_n| = |\dot{d}| = \mu|\chi| \leq \mu\overline{\chi},$$

$$|v_n^2 - V_n^2| \leq 2\overline{v}\mu\overline{\chi}, \quad \left|\sqrt{\overline{v}^2 - v_n^2} - \sqrt{\overline{v}^2 - V_n^2}\right| \leq \sqrt{2\overline{v}\mu\overline{\chi}}, \tag{C2}$$

$$\Rightarrow |v_\tau|^2 = \overline{v}^2 - v_n^2 \geq \overline{v}^2 - (|V_n| + \mu\overline{\chi})^2 \geq \overline{v}^2 - (\overline{v} - \Delta_v + \mu\overline{\chi})^2 \overset{(22)}{\geq} \overline{v}^2 - (\overline{v} - \Delta_v/2)^2$$
$$= \overline{v}\Delta_v - \Delta_v^2/4 > 0 \Rightarrow 1); \tag{C3}$$

$$|\gamma_\pm(d, \boldsymbol{\varrho}, t, v_n) - \gamma_\pm(d, \boldsymbol{\varrho}, t, V_n)| \overset{(4)}{\leq} \frac{|\varkappa||v_n^2 - V_n^2| + 2|\omega|\left|\sqrt{\overline{v}^2 - v_n^2} - \sqrt{\overline{v}^2 - V_n^2}\right|}{1 + \varkappa d}$$
$$\overset{\text{Assumption 3.2,(19), (C2)}}{\leq} \frac{2\overline{\varkappa}\,\overline{v}\,\overline{\chi}\mu + 2\overline{\omega}\sqrt{2\overline{v}\,\overline{\chi}\mu}}{\Delta_d},$$

$$\boldsymbol{u} \overset{(10)}{=} \boldsymbol{v}/\|\boldsymbol{v}\| = v_n/\overline{v}\,\boldsymbol{n} + \sigma_\tau\sqrt{1 - v_n^2/\overline{v}^2}\,\boldsymbol{\tau}, \text{ where } \sigma_\tau := \mathbf{sgn}\, v_\tau, \quad \boldsymbol{u}^\perp = -v_n/\overline{v}\,\boldsymbol{\tau} + \sigma_\tau\sqrt{1 - v_n^2/\overline{v}^2}\,\boldsymbol{n},$$

$$\dot{S} \overset{(4),(10),(A9)}{=\!=\!=} -\sigma\sigma_\tau \mathbf{sgn}\, S\left[\overline{a}\sqrt{1 - V_n^2/\overline{v}^2} + \sigma\sigma_\tau \mathbf{sgn}\, S\gamma_{\sigma_\tau}(d, \boldsymbol{\varrho}, t, V_n) - \theta\right], \tag{C4}$$

$$\text{where} \quad \theta := -\frac{\overline{a}}{\overline{v}}\sqrt{\overline{v}^2 - v_n^2} + \frac{\overline{a}}{\overline{v}}\sqrt{\overline{v}^2 - V_n^2} + \sigma\sigma_\tau \mathbf{sgn}\, S\left[\gamma_{\sigma_\tau}(d, \boldsymbol{\varrho}, t, v_n) - \gamma_{\sigma_\tau}(d, \boldsymbol{\varrho}, t, V_n) + \mu\chi'\dot{d}\,\right],$$

$$|\theta| \overset{(15),(C2)}{\leq} q := \frac{\overline{a}\sqrt{2\mu\overline{\chi}}}{\sqrt{\overline{v}}} + 2\frac{\overline{\varkappa}\,\overline{v}\,\overline{\chi}\mu + \overline{\omega}\sqrt{2\overline{v}\,\overline{\chi}\mu}}{\Delta_d} + \mu^2\overline{\chi}\,\overline{\chi}'.$$

By invoking Assumption 3.2, we see that in (C4), the expression in [. . .] is no less than $\Delta_a - q > 0$ by (22). Thus the sign of the limit from (C1) equals $-\sigma\sigma_\tau$. This and (C1) complete the proof. □

Lemma C2. *In mode $\mathfrak{R}$, the speed $v \equiv \overline{v}$ and within the time interval $[0, T := 3\pi\overline{v}/\overline{a}]$ the robot remains in the operational zone Z_{op} and arrives at a position where $S = \dot{d} + \mu\chi(d) = 0, \sigma v_\tau > 0$.*

Proof. By (10) and (1) in Assumption 3.5, $v \equiv \overline{v}$ and the robot moves over a circle C with a radius of $R = \overline{v}^2/\overline{a}$ and so, by (3) in Assumption 3.5, lies in Z_{op} until $t = T$ or $\mathfrak{R}$ is turned off. Thus, it remains to prove the last claim of the lemma, assuming that it is not true for $t = 0$.

Then $S \neq 0$ for $t > 0, t \approx 0$ thanks to Lemma C1 and (1) in Assumption 3.5. Let t_0 be the first time t when either (a) $S = 0$, or (b) $t = T$, or (c) mode $\mathfrak{R}$ is turned off. It suffices to show that in fact the event (a) holds at $t = t_0$.

To this end, we translate the line L from (2) in Assumption 3.5 toward $\boldsymbol{r}(0)$ by a distance of $3\pi\overline{v}^2/\overline{a}$. Since the speed of any point in Γ does not exceed $\overline{v}$ by (5), for $t \in [0, t_0]$, (d) $\Gamma(t)$ and C remain separated by L and (e) the distance from the robot to Γ exceeds $d_\downarrow$ due to (16). Hence, (c) does not hold by (9) and (e). Suppose that $t_0 = T$. Then by (d), the polar angle of the vector $\boldsymbol{r}(t) - \boldsymbol{\varrho}(t)$ continuously evolves over an interval whose length does not exceed π. Meanwhile, the polar angle of the velocity $\boldsymbol{v}(t)$ continuously runs over an interval with a length of 3π. Hence, there exist two instants $t_i \in [0, T]$, $i = 1, 2$ such that $\boldsymbol{v}(t_i)$ and $(-1)^i[\boldsymbol{\varrho}(t_i) - \boldsymbol{r}(t_i)]\,\mathbf{sgn}\, d(t_i)$ are co-linear and identically directed. Since $\boldsymbol{\varrho}(t_i) - \boldsymbol{r}(t_i)$ and $\boldsymbol{n}[\boldsymbol{\varrho}(t_i), t_i]\,\mathbf{sgn}\, d(t_i)$ are colinear and identically directed, we have $(-1)^{i+1}S(t_i) \overset{(A9)}{=} (-1)^{i+1}V_n(t_i) + (-1)^i\langle \boldsymbol{v}(t_i); \boldsymbol{n}[\boldsymbol{\varrho}(t_i), t_i]\rangle + (-1)^{i+1}\mu\chi = \overline{v} - (-1)^i[V_n(t_i) + \mu\chi] \overset{(15)}{\geq} \overline{v} - |V_n| - \mu\overline{\chi} \overset{\text{Assumption 3.2}}{\geq} \Delta_v - \mu\overline{\chi} \overset{(22)}{>} 0$. Thus, the continuous function of time S assumes values of opposite signs at $t = t_1, t_2$. It follows that S inevitably arrives at zero within $(0, t_0)$, in violation of the definition of t_0. Hence, $t_0 \neq T$ and so (a) does hold. □

https://doi.org/10.1017/S0263574721000667 Published online by Cambridge University Press

By Lemma C1, the sliding motion (SM) over the surface $\mathcal{S}$ commences at $t = t_0$ and then is maintained until the robot is in Z_{op} and mode $\mathfrak{R}$. During this motion, $\dot{d} = -\mu\chi(d)$ and so d monotonically goes to 0 due to (15). This and (2) guarantee that the robot cannot live Z_{op} during SM. As a result, we arrive at the following.

Corollary C1. *Mode $\mathfrak{R}$ does terminate; this occurs in a situation where the robot undergoes SM over the surface $\mathcal{S}$ with $\sigma v_\tau > 0$ and $v \equiv \overline{v}$ within Z_{op} and arrives at a distance of $d_\downarrow$ to Γ.*

Lemma C3. *While two robots $i \neq j$ are both in mode $\mathfrak{R}$, they cannot collide.*

Proof . Until time $T = 3\pi\overline{v}/\overline{a}$, every of them runs a distance $\leq \overline{v}T = 3\pi\overline{v}^2/\overline{a}$ and so collision is impossible thanks to (4) in Assumption 3.5. For $t \geq T$ and $k = i, j$, $\dot{d}_k = -\mu\chi(d_k)$, $v_k = \overline{v}$, and $\sigma v_{k,\tau} > 0$ by Lemmas C1 and C2. Hence, $d_i(T) \neq d_j(T) \Rightarrow d_i(t) \neq d_j(t)$ for $t \geq T$, which excludes the collision. If $d_i(T) = d_j(T)$, then $d_i(t) = d_j(t) =: d(t)$ for $t \geq T$. Then (A9) yields that $v_{k,n} = V_n - \dot{d}$, $v_{k,\tau} = \sigma\sqrt{\overline{v}^2 - (V_n - \dot{d})^2}$,

$$\dot{\boldsymbol{r}}_k \overset{(A8)}{=} [V_n(\boldsymbol{\varrho}_k, t) - \dot{d}(t)]\boldsymbol{n}(\boldsymbol{\varrho}_k, t) + \sigma\sqrt{\overline{v}^2 - [V_n(\boldsymbol{\varrho}_k, t) - \dot{d}(t)]^2}\boldsymbol{\tau}(\boldsymbol{\varrho}_k, t).$$

Thus $\boldsymbol{r}_i(t)$ and $\boldsymbol{r}_j(t)$ solve a common ODE, whereas $\boldsymbol{r}_i(T) \neq \boldsymbol{r}_j(T)$. Hence, $\boldsymbol{r}_i(t) \neq \boldsymbol{r}_j(t)$ for $t \geq T$. □

Corollary C2. *If two robots arrive at the triggering threshold $d_\downarrow$ simultaneously, they start mode $\mathfrak{T}$ from different positions and with different projections $\boldsymbol{\varrho}$ onto Γ.*

D. Proofs of (i)–(iv) in theorems 1 and 2: behavior in mode $\mathfrak{T}$

The assumptions of Theorem 2 are still considered as true. Now we study the behavior in mode $\mathfrak{T}$ with $\sigma = 1$; the case $\sigma = -1$ is treated likewise. The function $\Xi(\cdot)$ from (14) is extended on $\mathbb{R}$ by putting $\Xi(s) := \Xi(0)\ \forall s < 0$ and $\Xi(s) := \Xi(\Delta^s)$ for $s > \Delta^s$. We also put $S_i := \dot{d}_i + \mu\chi(d_i)$ and $\mathcal{S}_i := \{(\boldsymbol{r}_i, \boldsymbol{v}_i, t) : S_i = 0\}$.

Lemma D1. *The part $\mathcal{S}_{\downarrow,i}$ of $\mathcal{S}_i$ where $v_i \leq \overline{v}$ and $|d_i| \leq d_\downarrow$ is sliding.*

Proof . Let a point of the phase space of robot i goes to a certain point of $\mathcal{S}_{\downarrow,i}$ so that $S_i \neq 0$ and $\mathbf{sgn}\, S_i$ is kept unchanged. Due to (13) and (A9) and similarly to the proof of Lemma C1, we have

$$\lim \dot{S}_i \mathbf{sgn}\,(S_i) = -\overline{a}_n + \mathbf{sgn}\,(S_i)[\beta(v_{i,\tau}, d_i) - \mu^2\chi'\chi],$$

$$\text{where } \beta(\zeta, d) := \frac{\varkappa\zeta^2 + 2\zeta\omega - \omega^2 d}{1 + \varkappa d} - \varkappa V_\tau^2 - 2\omega V_\tau + A_n, \quad \text{(D1)}$$

$$\left|\beta(v_{i,\tau}, d_i) - \beta(v_{i,\tau}, 0)\right| = |d_i|(\omega + \varkappa v_{i,\tau})^2(1 + \varkappa d_i)^{-1} \overset{\text{Assumption 3.2,(19)}}{\leq} d_\downarrow(\overline{\omega} + \overline{\varkappa v})^2/\Delta_d,$$

$$|v_{i,\tau}| = \sqrt{v_i^2 - v_{i,n}^2} \overset{(A9)}{\leq} \sqrt{\overline{v}^2 - (V_n - \dot{d})^2} \leq \sqrt{\overline{v}^2 - V_n^2} + |V_n|\mu\overline{\chi}(\overline{v}^2 - V_n^2)^{-1/2},$$

$$|\beta(v_{i,\tau}, 0)| \overset{(19)}{\leq} \max_{0 \leq \zeta \leq \sqrt{\overline{v}^2 - V_n^2}} |\beta(\zeta, 0)| + 2|V_n|\mu\overline{\chi}\left[\left(1 + \frac{|V_n|\mu\overline{\chi}}{\overline{v}^2 - V_n^2}\right)\overline{\varkappa} + \frac{\overline{\omega}}{\sqrt{\overline{v}^2 - V_n^2}}\right]$$

$$\overset{\text{Assumption 3.2}}{\leq} \max_{0 \leq \zeta \leq \sqrt{\overline{v}^2 - V_n^2}} |\beta(\zeta, 0)| + 2\overline{v}\mu\overline{\chi}\left[\left(1 + \frac{\overline{v}\mu\overline{\chi}}{\Delta_v^2}\right)\overline{\varkappa} + \frac{\overline{\omega}}{\Delta_v}\right].$$

By invoking Assumption 3.2 and the relationship between the conditions from Lemma 2 and (B13) (which has been established in the proof of Lemma 2), we see that the last maximum $\leq \overline{a}_n - \Delta_a^n$.

https://doi.org/10.1017/S0263574721000667 Published online by Cambridge University Press

Hence

$$|\beta(v_{i,\tau}, d_i) - \mu^2\chi'\chi| \overset{(15)}{\leq} \overline{a}_n - \Delta_a^n + \frac{d_\downarrow}{\Delta_d}(\overline{\omega} + \overline{\varkappa v})^2 + 2\overline{v}\mu\overline{\chi}\left[\left(1 + \frac{\overline{v}\mu\overline{\chi}}{\Delta_v^2}\right)\overline{\varkappa} + \frac{\overline{\omega}}{\Delta_v}\right] + \mu^2\overline{\chi\chi'} \overset{(16),(22)}{<} \overline{a}_n.$$

So (D1) implies the first formula from (C1), which completes the proof. □

Remark D1. By the continuity argument, the above proof shows that $S_i \neq 0 \Rightarrow \mathbf{sgn}\, S_i \cdot \dot{S}_i < 0$ if the robot is in the domain $\mathcal{S}_{\downarrow,i}^{\delta_\Sigma}$ given by $|S_i| < \delta_\Sigma$, $v_i < \overline{v} + \delta_\Sigma$, $|d_i| < d_\downarrow + \delta_\Sigma$ and $\delta_\Sigma > 0$ is small enough.

By invoking Corollary C1 and noting that during SM $\dot{d}_i = -\mu\chi(d_i)$ and so d_i monotonically goes to 0 from $d_\downarrow$ by (15), thus keeping the claim $|d_i| \leq d_\downarrow$ from Lem. D1 true, we arrive at the following.

Corollary D1. *After robot i switches to mode $\mathfrak{T}$, it undergoes SM over $\mathcal{S}_i$ while $v_i \leq \overline{v} + \delta_\Sigma$.*

For a state $\boldsymbol{x} = \left[\{(\boldsymbol{r}_i, \boldsymbol{v}_i)\}_{i=1}^N, t\right]$ of the team, robot i is said to be *single* if $\boldsymbol{\varrho}_i \neq \boldsymbol{\varrho}_j \ \forall j \neq i$, and *multiple* otherwise. Also, $q^{\leftarrow}$ stands for any limit to which a quantity $q = q(\boldsymbol{x}')$ may converge as $\boldsymbol{x}' \to \boldsymbol{x}$. For single robots, $s_i^{\leftarrow} = s_i$, and $s_i^{\leftarrow} = s_i, 0$ for multiple ones.

Lemma D2. *Let* $\mathbf{sgn}\, 0 := 0$. *There is $\Delta_\Sigma > 0$ such that for any j and the map $\Sigma_i(s,t)$ from* (14),

$$\exists \gamma = \pm 1 \text{ such that } \gamma = \mathbf{sgn}\, \Sigma_i(s_i^{\leftarrow}, t)\ \forall s_i^{\leftarrow} \Rightarrow \gamma \frac{d}{dt}\Sigma_i(s_{i\to j}, t) \leq -\Delta_\Sigma \quad \text{if robot } i \text{ is on } \mathcal{S}_{\downarrow,i}. \tag{D2}$$

Proof . By (15) and (A9), $|v_{i,n} - V_n| \leq \mu\overline{\chi}$ on $\mathcal{S}_i$. For $V_{*,\tau} := \sqrt{\overline{v}^2 - V_n^2}$, $v_{*,\tau} := \sqrt{\overline{v}^2 - v_{i,n}^2}$, we see that

$$\left|v_{i,\tau} - V_{*,\tau}\right| \leq \frac{\mu\overline{\chi v}}{\sqrt{\overline{v}^2 - [|V_n| + \mu\overline{\chi}]^2}} \overset{(C3)}{\leq} \frac{\mu\overline{\chi v}}{\sqrt{\overline{v}\Delta_v - \Delta_v^2/4}}; \ \left|(|\omega| + |\varkappa|v_{*,\tau})|v_{i,n}| - (|\omega| + |\varkappa|V_{*,\tau})|V_n|\right|$$

$$\leq (|\omega| + |\varkappa|v_{*,\tau})|v_{i,n} - V_n| + |\varkappa||v_{*,\tau} - V_{*,\tau}||V_n| \overset{(5),(19)}{\leq} \mu(\overline{\omega} + \overline{\varkappa v})\overline{\chi} + \frac{\mu\overline{\varkappa\chi v}^2}{\sqrt{\overline{v}\Delta_v - \Delta_v^2/4}};$$

$$\left|(|\omega| + |\varkappa|v_{*,\tau})v_{*,\tau} - (|\omega| + |\varkappa|V_{*,\tau})V_{*,\tau}\right| \leq \left[|\omega| + |\varkappa|(v_{*,\tau} + V_{*,\tau})\right]|v_{*,\tau} - V_{*,\tau}|$$

$$\leq \frac{\mu\overline{\chi}(\overline{\omega} + 2\overline{\varkappa v})\overline{v}}{\sqrt{\overline{v}\Delta_v - \Delta_v^2/4}}; \qquad \left|\frac{v_{i,n}}{\sqrt{\overline{v}^2 - v_{i,n}^2}} - \frac{V_n}{\sqrt{\overline{v}^2 - V_n^2}}\right| \leq \frac{\mu\overline{v}^3\overline{\chi}}{(\overline{v}\Delta_v - \Delta_v^2/4)^{3/2}}.$$

By Fig. 1(b), $\vartheta_1 = 0$, $\vartheta_1' = 0$ whenever $|d_i| > \delta_2 d_\downarrow$. If conversely, $|d_i| \leq \delta_2 d_\downarrow$, we have

$$\left|\frac{\omega + \varkappa v_{i,\tau}}{1 + \varkappa d_i}\right| \overset{(19)}{\leq} \frac{\overline{\omega} + \overline{\varkappa v}}{1 - \overline{\varkappa} d_\downarrow}, |\dot{\mathfrak{s}}_i| \overset{(A8)}{\leq} \frac{\overline{v} + \overline{\omega}\delta_2 d_\downarrow}{1 - \overline{\varkappa} d_\downarrow}, |\dot{\omega}| \overset{(A12)}{\leq} \overline{\omega}' \frac{\overline{v} + \overline{\omega}\delta_2 d_\downarrow}{1 - \overline{\varkappa} d_\downarrow} + \epsilon, |\dot{\varkappa}| \leq \overline{\varkappa}' \frac{\overline{v} + \overline{\omega}\delta_2 d_\downarrow}{1 - \overline{\varkappa} d_\downarrow} + \overline{\wp}, \tag{D3}$$

$$\left|\frac{d}{dt}\left[\frac{\omega + \varkappa v_{i,\tau}}{1 + \varkappa d_i} d_i\right]\right| \overset{(A10)}{=} \left|\frac{(\omega + \varkappa v_{i,\tau})[\dot{d}_i - \dot{\varkappa} d_i^2]}{(1 + \varkappa d_i)^2} + \frac{\dot{\omega} + \dot{\varkappa} v_{i,\tau}}{1 + \varkappa d_i} d_i + \frac{\varkappa d_i}{1 + \varkappa d_i}\left[a_{i,\tau} + \frac{\omega + \varkappa v_{i,\tau}}{1 + \varkappa d_i} v_{i,n}\right]\right|$$

$$\leq \frac{(\overline{\omega} + \overline{\varkappa v})(\mu\overline{\chi} + \overline{\varkappa v} d_\downarrow)}{(1 - \overline{\varkappa} d_\downarrow)^2} + \left[\frac{(\overline{\omega} + \overline{\varkappa v})\overline{\varkappa}'(\overline{v} + \overline{\omega} d_\downarrow)d_\downarrow}{(1 - \overline{\varkappa} d_\downarrow)^3} + \frac{\epsilon}{1 - \overline{\varkappa} d_\downarrow} + \frac{(\overline{\wp} + \overline{\omega}' + \overline{v}\overline{\varkappa}')(\overline{v} + \overline{\omega} d_\downarrow)}{(1 - \overline{\varkappa} d_\downarrow)^2}\right]\delta_2 d_\downarrow$$

$$+ \frac{\overline{\varkappa} d_\downarrow \overline{a}}{1 - \overline{\varkappa} d_\downarrow} \overset{(17)}{\leq} \frac{(\overline{\omega} + \overline{\varkappa v})(\mu\overline{\chi} + \overline{\varkappa v} d_\downarrow)}{(1 - \overline{\varkappa} d_\downarrow)^2} + \frac{\overline{\varkappa} d_\downarrow \overline{a}}{1 - \overline{\varkappa} d_\downarrow} + \frac{\Delta_a^\tau}{6}.$$

https://doi.org/10.1017/S0263574721000667 Published online by Cambridge University Press

We then note that $a_i^{\tau,\leftarrow} = -\gamma \bar{a}_\tau - b_i^{\Sigma,\leftarrow}$ by (13) and the premises from (D2). Hence

$$\Sigma_i(s,t) \overset{\text{Fig. 1(b),(14),(A8)}}{=\!=\!=} v_{i,\tau} - \vartheta_1 \frac{\omega + \varkappa v_{i,\tau}}{1+\varkappa d_i} d_i - \left[\vartheta_3 \sqrt{\overline{v}^2 - v_{i,n}^2} + \vartheta_4 \Xi(s)\right];$$

$$\gamma \frac{d}{dt}\Sigma_i(s_{i\to j},t) \overset{(13),(14),(A10)}{=\!=\!=} -\bar{a}_\tau - \gamma A^{\leftarrow}, \quad \text{where } A^{\leftarrow} := \frac{\varkappa d_i(\omega + \varkappa v_{i,\tau})}{1+\varkappa d_i} v_{i,n}$$

$$-(\omega + \varkappa v_{i,\tau})v_{i,n} - \vartheta_3\left[\tfrac{d_i}{d_\downarrow}\right] \frac{v_{i,n}}{\sqrt{\overline{v}^2 - v_{i,n}^2}}\left[a_{i,n} + \frac{\varkappa d_i(\omega+\varkappa v_{i,\tau})}{1+\varkappa d_i} v_{i,\tau} - (\omega + \varkappa v_{i,\tau})v_{i,\tau}\right]$$

$$+\vartheta_4\left[\tfrac{d_i}{d_\downarrow}\right]\frac{d\Xi(s_{i\to j})}{dt} + \vartheta_3' \cdot \left[\frac{\dot{d}_i}{d_\downarrow}\sqrt{\overline{v}^2 - v_{i,n}^2} - \frac{\dot{d}_i}{d_\downarrow}\Xi(s_{i\to j})\right] + b_i^{\Sigma,\leftarrow}$$

$$+\vartheta_1' \dot{d}_i \frac{\omega + \varkappa v_{i,\tau}}{1+\varkappa d_i}\frac{d_i}{d_\downarrow} + \vartheta_1 \frac{d}{dt}\left[\frac{\omega+\varkappa v_{i,\tau}}{1+\varkappa d_i} d_i\right];$$

$$|A^{\leftarrow}| \overset{(14),(19),(21),(C3)}{\leq} \frac{\overline{\varkappa} d_\downarrow(\overline{\omega} + \overline{\varkappa v})\overline{v}}{1 - \overline{\varkappa} d_\downarrow} + (|\omega| + |\varkappa||v_{i,\tau}|)|v_{i,n}|$$

$$+\frac{v_{i,n}}{\sqrt{\overline{v}^2 - v_{i,n}^2}}\left[\overline{a}_n + \frac{\overline{\varkappa} d_\downarrow(\overline{\omega}+\overline{\varkappa v})\overline{v}}{1-\overline{\varkappa} d_\downarrow} + (|\omega| + |\varkappa||v_{i,\tau}|)|v_{i,\tau}|\right]$$

$$+\overline{\Xi}'|\dot{s}_{i\to j}| + \left[\frac{(\overline{v} + \overline{\Xi})\overline{\vartheta}_3'}{d_\downarrow} + \frac{(\overline{\vartheta}_1' + 1)(\overline{\omega} + \overline{\varkappa v})}{(1-\overline{\varkappa} d_\downarrow)^2}\right]\mu\overline{\chi} + \frac{(\overline{\omega} + \overline{\varkappa v})\overline{\varkappa v} d_\downarrow}{(1-\overline{\varkappa} d_\downarrow)^2} + \frac{\overline{\varkappa} d_\downarrow \overline{a}}{1-\overline{\varkappa} d_\downarrow} + \frac{\Delta_a^\tau}{6} + N\varkappa_b$$

$$\overset{(25),(C3),|v_{i,\tau}|\leq v_{*,\tau}}{\leq} \underbrace{(2(|\omega| + |\varkappa|V_{*,\tau})|V_n| + |V_n|\overline{a}_n(\overline{v}^2 - V_n^2)^{-1/2}}_{\leq \overline{a}_\tau - \Delta_a^\tau \text{ by Assumption 3.2}} + \overline{\Xi}'|\dot{s}_{i\to j}| + \frac{2\Delta_a^\tau}{6}$$

$$+\frac{\overline{\varkappa} d_\downarrow}{1-\overline{\varkappa} d_\downarrow}\left[\overline{a} + 2\frac{(\overline{\omega}+\overline{\varkappa v})\overline{v}}{1-\overline{\varkappa} d_\downarrow}\right]\left[1 + \frac{\overline{v}}{\sqrt{\overline{v}\Delta_v - \Delta_v^2/4}}\right]$$

$$+\left\{\frac{(\overline{v}+\overline{\Xi})\overline{\vartheta}_3'}{d_\downarrow} + \frac{\overline{v}^3[\overline{a}_n + (\overline{\omega} + \overline{\varkappa v})\overline{v}]}{(\overline{v}\Delta_v - \Delta_v^2/4)^{3/2}} + \frac{(\overline{\vartheta}_1' + 2)(\overline{\omega} + \overline{\varkappa v})}{(1-\overline{\varkappa} d_\downarrow)^2}\right.$$

$$\left. + \left[\overline{\varkappa} + \frac{(\overline{\omega} + 2\overline{\varkappa v})}{\sqrt{\overline{v}\Delta_v - \Delta_v^2/4}}\right]\frac{\overline{v}^2}{\sqrt{\overline{v}\Delta_v - \Delta_v^2/4}}\right\}\mu\overline{\chi}.$$

By (18), (23), the fourth and fifth addends are less than $\Delta_a^\tau/6$. By (5), (19), (A7), and (A8), $|\dot{s}_{i\to j}(t)| \leq 2(\overline{v} + \overline{\omega} d_\downarrow)/(1-\overline{\varkappa} d_\downarrow) + \overline{p}\,\overline{\varkappa}\,\overline{v}$ and so $\overline{\Xi}'|\dot{s}_{i\to j}| < \Delta_a^\tau/6$ by (21). Overall, $|A| \leq \overline{a}_\tau - \Delta_a^\tau/6$. The proof of (D2) is completed by bringing the pieces together. □

Remark D2. By the above proof, (D2) remains true if $s_{i\to j}(\cdot)$ is replaced by any function $s(\cdot)$ such that

$$|\dot{s}| \leq 2(\overline{v} + \overline{\omega} d_\downarrow)/(1-\overline{\varkappa} d_\downarrow) + \overline{p}\,\overline{\varkappa}\,\overline{v} \tag{D4}$$

and in (14), $\Xi(\cdot)$ is replaced by any function $\Xi_*(\cdot)$ such that $|\Xi_*(s)| \leq \overline{\Xi}$ and $|\Xi_*'(s)| \leq \overline{\Xi}'$ for all s.

Remark D3. By the continuity argument, the entailment from (D2) (possibly with a lesser $\Delta_\Sigma > 0$) remains true provided that the robot is in $\mathcal{S}_{\downarrow,i}^{\delta_\Sigma}$ and $\delta_\Sigma > 0$ is small enough.

https://doi.org/10.1017/S0263574721000667 Published online by Cambridge University Press

Lemma D3. *In mode $\mathfrak{T}$, SM over $\mathcal{S}_i$ holds, $v_i < \overline{v}$, $|d_i| < d_\downarrow$, $\|\boldsymbol{a}_i\| \leq \overline{a}$, and $\Sigma_i(0,t) \geq 0$, $\Sigma_i(\Delta^s, t) \leq 0$.*

Proof . Let $t=0$ be assigned to the time when $\mathfrak{T}$ commences. By the continuity argument, robot i remains in the set $\mathcal{S}^{\delta\Sigma}_{\downarrow,i}$ from Remarks D1 and D3 for some time period $[0,t_*], t_*>0$ thanks to Corollary C1. With regard to Remark D2, we see that $\Sigma_i(\Delta^s,t)>0 \Rightarrow \Sigma_i(s_i^{\leftarrow},t)>0 \Rightarrow \frac{d}{dt}\Sigma_i(\Delta^s,t)<0$ and $\Sigma_i(0,t)<0 \Rightarrow \Sigma_i(s_i^{\leftarrow},t)<0 \Rightarrow \frac{d}{dt}\Sigma_i(0,t)>0$. Since $\Sigma_i(\Delta^s,0)\leq 0$ and $\Sigma_i(0,0)\geq 0$ by (14), (20), and (C1), we infer that $\Sigma_i(0,t)\geq 0$, $\Sigma_i(\Delta^s,t)\leq 0\ \forall t\in(0,t_*]$. Then if $d_i \geq \delta_2 d_\downarrow$,

$$|v_{i,\tau}| \overset{(14)}{\leq} \vartheta_3\sqrt{[\overline{v}^2 - v_{i,n}^2]_+} + \vartheta_4 \Xi(\Delta^s), \quad \text{where } \Xi(\Delta^s) \overset{(20),(C3)}{<} \sqrt{\overline{v}^2 - v_{i,n}^2} \quad \text{and } \vartheta_4 = 1-\vartheta_3 \in (0,1]$$

by Fig. 1(b). It follows that $v_i^2 = v_{i,n}^2 + v_{i,\tau}^2 < \overline{v}^2$ for $t\in(0,t_*]$. If $d_i \leq \delta_2 d_\downarrow$, we have due to Fig. 1(b),

$$\Xi(\Delta^s) \overset{(14)}{\geq} \vartheta_1\dot{\mathfrak{s}}_i + \vartheta_2 v_{i,\tau} \overset{(A8)}{=} v_{i,\tau} - \vartheta_1\frac{\omega + \varkappa v_{i,\tau}}{1+\varkappa d_i} d_i \overset{(D3)}{\Rightarrow} |v_{i,\tau}| \leq \Xi(\Delta^s) + \frac{\overline{\omega} + \overline{\varkappa v}}{1-\overline{\varkappa} d_\downarrow}\delta_2 d_\downarrow$$

$$\overset{(18),(20),(C3)}{<} \sqrt{\overline{v}^2 - v_{i,n}^2} \Rightarrow v_i < \overline{v}\ \forall t\in(0,t_*].$$

Thus, robot i undergoes SM over $\mathcal{S}_i$ for $t\in[0,t_*]$ by Lemma D1. Then $\dot{d}_i = -\mu\chi(d_i)$ and so d_i monotonically goes to 0 by (15), thus remaining in $[-d_\downarrow, d_\downarrow]$. Hence, the conclusion of the lemma holds on any interval $[0,t_*)$ during which the robot does not leave $\mathcal{S}^{\delta\Sigma}_{\downarrow,i}$. Let $[0,t_*)$ be a maximal such an interval. Suppose that $t_*<\infty$. By the foregoing, the robot is in fact in the closed manifold $\mathcal{S}_{\downarrow,i}$ for $t\in[0,t_*]$ and so remains in the open set $\mathcal{S}^{\delta\Sigma}_{\downarrow,i}$ a bit longer, in violation of the definition of t_*. This contradiction shows that $t_*=\infty$.

The proof of the lemma is completed by noting that due to (12)–(14), (25), and Fig. 1(a), we have $\|\boldsymbol{a}_i\|^2 \leq \overline{a}_n^2 + (\overline{a}_\tau + N\varkappa_b)^2 \leq \overline{a}_n^2 + \overline{a}_\tau^2 + 2N\overline{a}\varkappa_b + N^2\varkappa_b^2 \leq \overline{a}^2$. □

Corollary D2. *Any robot i goes to the targeted curve $d_i \to 0$ as $t\to\infty$, while d_i decays in mode $\mathfrak{T}$. If robots i and j commence mode $\mathfrak{T}$ simultaneously, then $d_i \equiv d_j$ in this mode; otherwise, $d_i \neq d_j$ at any time within $\mathfrak{T}$.*

Lemma D4. *If $s_{i\to j}\geq 0$ and $\Sigma_i(s_{i\to j},t)\leq 0$ at $t=t_*$, then $\Sigma_i(s_{i\to j},t)\leq 0$ for $t\geq t_*$ while $s_{i\to j}\geq 0$.*

Proof . We examine $t\geq t_*$ from an interval on which $s_{i\to j}\geq 0$. For $\eta(t) := \Sigma_i[s_{i\to j}(t),t]$, we have $\eta>0 \Rightarrow \Sigma_i[s_i^{\leftarrow},t]>0$ by (14) and (20). So $\dot{\eta}(t)<0$ by (D2). For $\eta_+(t) := \max\{\eta(t);0\}$, the Danskin theorem [30] yields that $\dot{\eta}_+(t)=0$ if $\eta_+(t)\leq 0$ and $\dot{\eta}_+(t)=\dot{\eta}(t)<0$ if $\eta_+(t)>0$. Overall, $\dot{\eta}_+(t)\leq 0$ a.e. and $\eta_+(t_*)=0$, which implies the conclusion of the lemma.

Lemma D5. *(i) Let robots $i\neq j$ commence mode $\mathfrak{T}$ simultaneously. Then $\boldsymbol{\varrho}_i \neq \boldsymbol{\varrho}_j$ throughout the duration of this mode. (ii) If $s_{i\to j}>0$, $\Sigma_i(s_{i\to j},t)\leq 0$, and $d_i, d_j < \delta_1 d_\downarrow$ at $t=t_*$, then $s_{i\to j}>0$ afterward.*

Proof . (i) Suppose the contrary. Let $t_=$ be the least time when the projection of one of these robots, say i, catches up to the projection of the other j. Further in this proof, $t<t_=, t\approx t_=$. For such t's, we have

$$s_{i\to j}(t)>0 \quad \text{and} \quad s_{i\to j}(t_=)=0. \tag{D5}$$

By (14), Fig. 1(b) and Corollary C1, C2, $\Sigma_i[s_{i\to j}(t),t]=0$ and $\boldsymbol{\varrho}_i\neq\boldsymbol{\varrho}_j$ at $t=0$. Since $t_=$ is the first time when $\boldsymbol{\varrho}_i=\boldsymbol{\varrho}_j$, (D5) implies that $s_{i\to j}$ continuously evolves from $s_{i\to j}(0)>0$ to 0 at time $t_=$. Then Lemma D4 guarantees that for $t\in[0,t_=]$,

$$\Sigma_i[s_{i\to j}(t),t]\leq 0 \overset{(14),(A8)}{\Longleftrightarrow} \dot{\mathfrak{s}}_i(1+\vartheta_2\varkappa d_i) + \vartheta_2\omega d_i \leq \vartheta_3\sqrt{\overline{v}^2 - v_{i,n}^2} + \vartheta_4\Xi(s_{i\to j}).$$

https://doi.org/10.1017/S0263574721000667 Published online by Cambridge University Press

By Lemma D3, $0 \le \Sigma_j(0,t) = \dot{\mathfrak{s}}_j(1+\vartheta_2\varkappa d_j) + \vartheta_2\omega d_j - \left[\vartheta_3\sqrt{\overline{v}^2 - v_{j,n}^2} + \vartheta_4\Xi(0)\right]$. Since $d_i \equiv d_j$ by Corollary D2, the quantities ϑ_k assume common values for robots i and j in mode $\mathfrak{T}$. By Assumption 3.3, (19) holds for $q := V$. So thanks to (A7) and (A8),

$$\dot{s}_{i\to j} \ge \frac{\vartheta_3\sqrt{\overline{v}^2 - v_{j,n}^2} + \vartheta_4\Xi(0) - \vartheta_2\omega(\boldsymbol{\varrho}_j,t)d_j}{1+\vartheta_2\varkappa(\boldsymbol{\varrho}_j,t)d_j} - \frac{\vartheta_3\sqrt{\overline{v}^2 - v_{i,n}^2} + \vartheta_4\Xi(s_{i\to j}) - \vartheta_2\omega(\boldsymbol{\varrho}_i,t)d_i}{1+\vartheta_2\varkappa(\boldsymbol{\varrho}_i,t)d_i} - \overline{\varkappa}\overline{V}s_{i\to j}. \tag{D6}$$

$$\left|\sqrt{\overline{v}^2 - v_{i,n}^2(t)} - \sqrt{\overline{v}^2 - v_{j,n}^2(t)}\right| \overset{(A9)}{=} \left|\sqrt{\overline{v}^2 - [V_n(\boldsymbol{\varrho}_i) - \mu\chi(d_i)]^2} - \sqrt{\overline{v}^2 - [V_n(\boldsymbol{\varrho}_j) - \mu\chi(d_i)]^2}\right|$$

$$\overset{(C3)}{\le} \frac{\overline{V}+\mu\overline{\chi}}{\sqrt{\overline{v}\Delta_v - \Delta_v^2/4}}\|V(\boldsymbol{\varrho}_i) - V(\boldsymbol{\varrho}_j)\| \le c_V\frac{\overline{V}+\mu\overline{\chi}}{\sqrt{\overline{v}\Delta_v - \Delta_v^2/4}}s_{i\to j}.$$

Here we use that by Assumptions 2.1, 3.3, any $f(\boldsymbol{\varrho},t) := \varkappa(\boldsymbol{\varrho},t), \omega(\boldsymbol{\varrho},t), V(\boldsymbol{\varrho},t)$ is t-uniformly Lipschitz continuous:

$$|f(\boldsymbol{\varrho}_i,t) - f(\boldsymbol{\varrho}_j,t)| \le c_f s_{i\to j}. \tag{D7}$$

By using these, we also infer that

$$\dot{s}_{i\to j} \ge \frac{\vartheta_4[\Xi(0) - \Xi(s_{i\to j})]}{1+\vartheta_2\varkappa(\boldsymbol{\varrho}_j,t)d_i} - \Omega s_{i\to j}, \tag{D8}$$

for some $\Omega \in (0,\infty)$. Meanwhile, $s^0(t) \equiv 0$ solves the ODE that results from the substitution $\ge\mapsto=$ in (D8). Then $\exists t < t_=: s_{i\to j}(t) > s^0(t) \Rightarrow s_{i\to j}(t_=) > s^0(t_=) = 0$ by [31, Theorem 4.1, Chapter 3], in violation of (D5). This contradiction completes the proof.

(ii) Suppose the contrary. Let $t_=$ be the least time $t > t_*$ when $s_{i\to j} = 0$; then (D5) still holds. For $t \ge t_*$, we have $d_i, d_j < \delta_1 d_\downarrow$ by Corollary D2 and so $\Sigma_i(s_{i\to j},t) = \dot{\mathfrak{s}}_i - \Xi(s_{i\to j}) \le 0\ \forall t \in [t_*, t_=)$ by (14), Fig. 1(b), and Lemma D4, whereas $\Sigma_j(0) = \dot{\mathfrak{s}}_j - \Xi(0) \ge 0$ by Lemma D3. Then (D6), (D8) take the form: $\dot{s}_{i\to j} \ge \Xi(0) - \Xi(s_{i\to j}) - \overline{\varkappa}\overline{V}s_{i\to j}$. This implies violation of (D5), as has just been shown. This contradiction proves **(ii)**. □

By gathering Lemmas C2, C3, D3, D5 and Corollary D2 and invoking (16), we arrive at the following.

Corollary D3. *The claims 1–3 from Theorem 1 hold.*

Hence there is time $t_\dagger$ such that for $t \ge t_\dagger$, all robots are in mode $\mathfrak{T}$, and for any robot i,

$$|\lambda_i - \omega V_n| \overset{(A12)}{<} \delta_b/8\ \forall k, \qquad |d_i| < \delta_1 d_\downarrow \quad \text{and so} \quad \Sigma_i(s,t) = \dot{\mathfrak{s}}_i - \Xi(s) \text{ by (14) and Fig. 1(b).} \tag{D9}$$

where δ_b and δ_1 are taken from Fig. 1. In the remainder of this section, $t \ge t_\dagger$. Then the system's state $\left[\boldsymbol{x}(t) = \{(\boldsymbol{r}_i, \boldsymbol{v}_i)\}_{i=1}^N, t\right]$ lies in the open set $\mathfrak{X} := \{(\boldsymbol{x},t): |d_i| < d_\downarrow, |\dot{d}_i + \mu\chi(d_i)| < \delta_\Sigma\ \forall i\}$, where δ_Σ is taken from Remark D1. The sentence following Assumption 3.3, (16), and (A8) imply that in $\mathfrak{X}$, another set of independent coordinates $\boldsymbol{y} = \left[\{(d_i, \dot{d}_i, \boldsymbol{\varrho}_i \in \Gamma(t), \dot{\mathfrak{s}}_i)\}_{i=1}^N, t\right]$ can be used since $\boldsymbol{x}$ and $\boldsymbol{y}$ are in a one-to-one smooth correspondence. In $\mathfrak{X}$, we introduce the surfaces $\mathfrak{S}_d$ and $\mathfrak{S}_{i,j}, i \ne j$ of states for which $\dot{d}_k + \mu\chi(d_k) = 0, v_{k,\tau} > 0 \forall k$ and $\boldsymbol{\varrho}_i = \boldsymbol{\varrho}_j$, respectively. By Lemma D3, the system moves over $\mathfrak{S}_d$ for $t \ge t_\dagger$.

Lemma D6. *Let* $[\boldsymbol{x}(t), t] \in \mathfrak{S}_d^{\text{sep}} := \mathfrak{S}_d \setminus \bigcup_{i\ne j}\mathfrak{S}_{i,j}\ \forall t \in [t_-, t_+)$. *Then the following claims hold:*

(i) *This trajectory is uniquely determined by its initial state at $t = t_-$ and smoothly depends on this state;*
(ii) *If $\dot{\mathfrak{s}}_i(t_*) = \Xi[s_i(t_*)]$ for some $t_* \in [t_-, t_+)$, SM over the surface $\dot{\mathfrak{s}}_i = \Xi(s_i)$ is going on for $t \in [t_*, t_+)$;*
(iii) *If $\dot{\mathfrak{s}}_i(t_*) \le \Xi[s_i(t_*)]$ for some $t_* \in [t_-, t_+)$ and i, robot i cannot catch up to its predecessor on $[t_*, t_+]$.*

https://doi.org/10.1017/S0263574721000667 Published online by Cambridge University Press

Proof . Claim (ii) follows from Lemma D2; (i) follows from (ii), (13), Lemma D3, and [27, Section 11, Chapter 2]. Claim (iii) is established by retracing the arguments from the proof of Lemma D5 and observing that now $\vartheta_2 = \vartheta_3 = 0, \vartheta_4 = 1$ in (D6), (D8) due to Fig. 1(b). □

Lemma D7. *(i) From any state in $\mathfrak{S}_d^{\rm m} := \mathfrak{S}_d \setminus \mathfrak{S}_d^{\rm sep}$ and at any $t_0 \geq t_\dagger$, a trajectory emerges that lies in $\mathfrak{S}_d^{\rm sep}$ for $t > t_0, t \approx t_0$. (ii) The last paragraph in Section 4 excludes the other emerging trajectories from consideration.*

Proof . (i) Let us consider such a state. We enumerate the robots in the counterclockwise order of their projections $\boldsymbol{\varrho}_i$ in that state, within every group I_l with common $\boldsymbol{\varrho}_i$'s (if exists), in the ascending order of $\dot{\mathfrak{s}}_i$, and within every group with common $\boldsymbol{\varrho}_i$'s and $\dot{\mathfrak{s}}_i$'s (if exists) arbitrarily. From that state, we launch the system driven by the law (12)–(14) modified via $s_i := s_{i\to i\oplus 1}$ in (13) and (14), $\Xi(z) := \Xi(0), b(z) := 1\ \forall z \leq 0$ and $\Xi(z) := \Xi(\Delta^s)\ \forall z \geq \Delta^s$, whereas the just established enumeration is used when counting the last sum in (14). By retracing the proof of Lemma D6, we see that for $t > t_0, t \approx t_0$, the respective trajectory $\mathfrak{t}$ exists, is unique, and meets (ii) from Lemma D6. For such t's, the groups I_l with various l's retain their order on $\Gamma(t)$ with respect to one another by the continuity argument. Within every group I_l, the subgroups J_* with a common $\dot{\mathfrak{s}}_i$ at $t = t_0$ become lined up in the ascending order of $\dot{\mathfrak{s}}_i$'s since $\dot{s}_{i\to j} = \dot{\mathfrak{s}}_j - \dot{\mathfrak{s}}_i$ at $t = t_0$ by (A7). Finally, we consider a subgroup J_* with more than one element.

Suppose first that $\dot{\mathfrak{s}}_i(t_0) > \Xi(0)\ \forall i \in J_*$. Then for $j := i \oplus 1$ and any $i \in J_m$ except for the maximal one, $\dot{\mathfrak{s}}_i(t) > \Xi[s_{i\to j}(t)]$ by the continuity argument. We also note that (19) holds for $\mathfrak{A}$ from (A11) and $s := \dot{s}_{i\to j}$, $\forall i, j$, and (D7) holds for $f := \omega V_n$. So

$$\ddot{s}_{i\to j} \overset{(12),(14),\,(A11),\,(D9),\,\text{Fig. }1(a)}{=\!=\!=} -\bar{a}_\tau \cdot \mathbf{sgn}\left[\dot{\mathfrak{s}}_j - \Xi(s_{j\to j\oplus 1})\right] + \bar{a}_\tau \cdot \mathbf{sgn}\left[\dot{\mathfrak{s}}_i - \Xi(s_{i\to j})\right] + b_i^\Sigma - b_j^\Sigma + \lambda_j - \lambda_i - \oint_{\varrho_i}^{\varrho_j} \mathfrak{A}\, ds \quad \text{(D10)}$$

$$\geq \varkappa_b/4 - |\omega(\boldsymbol{\varrho}_j, t)V_n(\boldsymbol{\varrho}_j, t) - \omega(\boldsymbol{\varrho}_i, t)V_n(\boldsymbol{\varrho}_i, t)| - \overline{\mathfrak{A}}|s_{i\to j}| \geq \varkappa_b/4 - (c_{\omega V_n} + \overline{\mathfrak{A}})|s_{i\to j}|$$

$$\geq \varkappa_b/8 \Rightarrow s_{i\to j}(t) \geq \varkappa_b(t - t_0)^2/16 > 0 \text{ if } t < t_0 + \eta, \text{ where } \eta := \varkappa_b[8\bar{s}(c_{\omega V_n} + \overline{\mathfrak{A}})]^{-1}. \quad \text{(D11)}$$

Now suppose that $\dot{\mathfrak{s}}_i(t_0) = \Xi(0)\ \forall i \in J_* = \{k, k\oplus 1, \ldots, m\}$. Since $\mathfrak{t}$ meets (ii) in Lemma D6, $\dot{\mathfrak{s}}_i = \Xi(s_{i\to i\oplus 1})\ \forall i \in J_*$ and so

$$\dot{s}_{m\ominus 1\to m} \overset{(19),\,(A7)}{=} \underbrace{\Xi(s_{m\to m\oplus 1}) - \Xi(0)}_{g} - \left[\Xi(s_{m\ominus 1\to m}) - \Xi(0)\right] - \overline{\varkappa}\overline{V}_n|s_{m\ominus 1\to m}|$$

$$\overset{(21)}{\geq} g - \alpha|s_{m\ominus 1\to m}|, \quad \text{where } \alpha := \overline{\Xi}' + \overline{\varkappa}\overline{V}_n. \quad \text{(D12)}$$

Then $s_{m\ominus 1\to m} \geq s$ by [31, Theorem 4.1, Chapter 3], where $s(t) = e^{-\alpha(t-t_0)}s_{m\ominus 1\to m}(t_0) + \int_{t_0}^t e^{-\alpha(t-\tau)}g(\tau)\, d\tau$ is the solution of the ODE $\dot{s} = -\alpha|s|$ at least while $s_{m\to m\oplus 1} > 0$. Hence, $s_{m\ominus 1\to m} > 0$ for $t > t_0$ and while $s_{m\to m\oplus 1} > 0$. This permits us to retrace (D12) for $m := m \ominus 1$, then for $m := m \ominus 2$, and so on until $m = k$.

Thus, all $\boldsymbol{\varrho}_i$'s are pair-wise distinct and arranged counterclockwise in any case. Hence, $\boldsymbol{\varrho}_{i\oplus 1}$ is the immediate predecessor of $\boldsymbol{\varrho}_i$. So $s_i = s_{i\to i\oplus 1}$, and the modified law is identical to the original one. This completes the proof of the first claim of the lemma.

(ii) Suppose that this claim is not true and consider a respective trajectory $\mathfrak{t}$. Suppose also that $\boldsymbol{\varrho}_i \neq \boldsymbol{\varrho}_j$ at individual times $t > t_0$ that are arbitrarily close to t_0. Then $\boldsymbol{\varrho}_i \neq \boldsymbol{\varrho}_j\ \forall t \in (t_0, t_0 + \varepsilon)$ for a small enough $\varepsilon > 0$. Indeed, suppose the contrary. Then arbitrarily close to t_0, there exists an interval (t_-, t_+) such that $t_- > t_0, \boldsymbol{\varrho}_i(t_\pm) = \boldsymbol{\varrho}_j(t_\pm)$, and $\boldsymbol{\varrho}_i(t) \neq \boldsymbol{\varrho}_j(t)\ \forall t \in (t_-, t_+)$; let $s_{i\to j} > 0\ \forall t \in (t_-, t_+)$ for the definiteness. Then $\dot{\mathfrak{s}}_i > \Xi(s_{i\to j}) \geq \Xi(s_i)\ \forall t \in (t_-, t_+)$ by (20), (D9), and (ii) in Lemma D5, whereas $\dot{s}_{i\to j}(t_-) \geq 0$. Hence by retracing (D10), we see that $\ddot{s}_{i\to j} = -\bar{a}_\tau \cdot \mathbf{sgn}\left[\dot{\mathfrak{s}}_j - \Xi(s_j)\right] + \bar{a}_\tau \cdot \mathbf{sgn}\left[\dot{\mathfrak{s}}_i - \Xi(s_i)\right] + b_i^\Sigma - b_j^\Sigma + \lambda_j - \lambda_i - \oint_{\varrho_i}^{\varrho_j} \mathfrak{A}\, ds \geq \varkappa_b/8$, $s_{i\to j}(t_+) = s_{i\to j}(t_-) + \dot{s}_{i\to j}(t_-)(t_+ - t_-) + \int_{t_-}^{t_+} \ddot{s}_{i\to j}(\tau)\, d\tau \geq \varkappa_b(t_+ - t_-)^2/16 > 0$, in violation of the above equation $s_{i\to j}(t_+) = 0$.

Hence, there is an interval $T := (t_0, t_0 + \varepsilon]$, $\varepsilon > 0$ such that if $i \neq j$, either $\boldsymbol{\varrho}_i \equiv \boldsymbol{\varrho}_j$ on T or $\boldsymbol{\varrho}_i \neq \boldsymbol{\varrho}_j$ on T. The definition of $\mathfrak{t}$ means that (i, j) of the first type exists. We are going to show that the trajectory $\mathfrak{t}$ is unviable. It suffices to do so provided that t_0 is subjected to an arbitrarily small increase. Then the set of robots can be arranged into groups such that $\boldsymbol{\varrho}_i \equiv \boldsymbol{\varrho}_j$ within a common group and $\boldsymbol{\varrho}_i \neq \boldsymbol{\varrho}_j\ \forall [t_0, t_0 + \varepsilon]$ if i and j are from different groups. The total size of the groups with size ≥ 2 is called the *degree* of the trajectory $\mathfrak{t}$. We are going to show that any trajectory of degree $m \geq 2$ is unviable, arguing via induction on m.

Let $m = 2$. Via a re-enumeration of the robots, if necessary, we ensure that $\boldsymbol{\varrho}_0 \equiv \boldsymbol{\varrho}_1$ (and so $\dot{s}_{0\to 1}(t_0) = 0$) and $\boldsymbol{\varrho}_i \neq \boldsymbol{\varrho}_{i\oplus 1}$, $i = 1, \dots, N-1$ on T. Almost all small perturbations of the state result in $\dot{\mathfrak{s}}_0 \neq \dot{\mathfrak{s}}_1$ and $\boldsymbol{\varrho}_0 \neq \boldsymbol{\varrho}_1$ at $t = t_0$; via re-enumeration, it can be ensured that $s_{0\to 1}(t_0) > 0$. In (D10) with $i := 0, j := 1$, now $s_{j\to j\oplus 1} \geq s_{i\to j} + \eta \forall t \in T$ if $\varepsilon \approx 0$, where $\eta > 0$ does not depend on t, ε. Hence, the sum of the first two addends from (D10) is nonnegative and so while $s_{i\to j} > 0$,

$$\ddot{s}_{i\to j} \geq \varkappa_b/4, \quad \dot{s}_{i\to j}(t) \geq \dot{s}_{i\to j}(t_0) + \varkappa_b(t - t_0)/4,$$
$$s_{i\to j}(t) \geq s_{i\to j}(t_0) + \dot{s}_{i\to j}(t_0)(t - t_0) + \varkappa_b(t - t_0)^2/8. \tag{D13}$$

Hence, if (a) $\dot{s}_{0\to 1}(t_0) \geq 0$, the perturbed trajectory goes away from $\mathfrak{t}$ on T. Let $\dot{s}_{0\to 1}(t_0) < 0$. Then $s_{0\to 1} > 0$ for all $t \in T$ if either $\dot{s}_{0\to 1}(t_0) \geq 0$ or $D := \dot{s}_{0\to 1}(t_0)^2 - \varkappa_b s_{0\to 1}(t_0)/2 < 0$; otherwise, for all $t \in (t_0, t_0 + \min\{\varepsilon, \delta\}$, where $\delta := -[4\dot{s}_{0\to 1}(t_0) + \sqrt{D}]/\varkappa_b$. So the following cases may occur. (b) $\dot{s}_{0\to 1}$ changes the sign at $t = t_\star \approx t_0$ and before $s_{0\to 1}$ does so. At $t = t_\star$, we have the case (a) and so still infer that $\mathfrak{t}$ is unstable. (c) $s_{0\to 1}$ changes the sign at $t = t_\star \approx t_0$ and before $\dot{s}_{0\to 1}$ does so. Via the re-enumeration $0 \leftrightarrows 1$ at $t = t_*$, we arrive at (a) once more. (d) $s_{0\to 1}$ and $\dot{s}_{0\to 1}$ simultaneously reach 0 at $t = t_\star \approx t_0$. While $s_{0\to 1} > 0$, the motion of robot 0 is identical to that generated by the modified control law. Now we examine a perturbation $s_1(t_0) + \eta$, $\eta \approx 0$ of the initial state. By [27, Section 11], the resultant deviation of the overall trajectory is Lipschitz in η. It follows that on T, the perturbation of $s_{0\to 1}$ has the form $\eta s + \zeta(t)$, where $|\zeta(t)| \leq \Upsilon\varepsilon$ and Υ does not depend on ε. So by picking ε small enough, we can ensure that the perturbation of $s_{0\to 1}$ has the order η uniformly on T. Since for the unperturbed $s_{0\to 1}$, the time derivative is zero at its root t_*, we infer that even if the root $t_*^\sim$ survives perturbation, $|t_*^\sim - t_*| \sim \sqrt{|\eta|}$. Similarly, the root of $\dot{s}_{0\to 1}$ is Lipschitz in η. Hence, these two roots do not coincide for $\eta \approx 0, \eta \neq 0$. So the case (d) does not hold for almost all perturbations of the state and $\mathfrak{t}$ is unviable.

Now let any trajectory of degree between 2 and m be unviable, and let $\mathfrak{t}$ be a trajectory of degree $m + 1$. Let I be any group of $m + 1$ robots that are colocated during T. At $t = t_0$, we slightly perturb the system's state so that all robots become separated. Let j be the leading robot in I. On the time interval $T_{\to j} \subset T$ where j still leads I, the arguments from the first part of the proof of (ii) show that (D13) holds for any $i \in I_{j\downarrow} := I \setminus \{j\}$. Hence if (a) $I_- := \{i \in I_{j\downarrow} : \dot{s}_{i\to j}(t_0) < 0\} = \emptyset$, the perturbed trajectory goes away from $\mathfrak{t}$ on T. Otherwise, $\dot{s}_{i\to j}(t) > 0\ \forall i \in T_{j\downarrow}$ no later than $t_* := t_0 + 4/\varkappa_b \max_{i\in I_-} |\dot{s}_{i\to j}(t_0)|$ unless j is overtaken earlier. If the last event does not occur, we face (a) at $t = t_*$ and so infer that $\mathfrak{t}$ is unstable. Suppose that it occurs; let t_* be the respective time. If on (t_0, t_*), some two robots from I become "stuck together", the degree of the perturbed trajectory lies between 2 and m. Hence, it is unviable by the induction hypothesis, and so is the initial trajectory as well. Suppose that on (t_0, t_*), no two robots from I "stuck together". By retracing the concluding arguments from the previous paragraph, we see that for almost all perturbations, the former leader j is overtaken by a single robot $i \in I_-$ and with nonzero relative speed. So the change of the leader reduces I_- by no less than one element. By continuing likewise, we infer instability of $\mathfrak{t}$ either at some step due to the above "stuck together" effect or after finitely many changes of the leader due to inevitably arriving at a) because of reduction in I_-. □

https://doi.org/10.1017/S0263574721000667 Published online by Cambridge University Press

Lemma D8. *For any considered trajectory, the times $t \geq t_\dagger$ when the state is in $\mathfrak{S}_d^{\mathrm{m}}$ do not accumulate.*

Proof . Suppose the contrary. By taking into account Lemma D7, this implies existence of a sequence $t_\dagger = t_0 < t_1 < t_2 < \ldots$ and a pair $i \neq j$ such that $\exists t_* = \lim_{k\to\infty} t_k < \infty$ and $\boldsymbol{\varrho}_i(t_k) = \boldsymbol{\varrho}_j(t_k)\ \forall k$, whereas $\boldsymbol{\varrho}_i(t) \neq \boldsymbol{\varrho}_j(t)\ \forall t \in (t_k, t_{k+1})$. From now on, k is large enough. The distance $s_{i\to j}$ keeps its sign unchanged on (t_k, t_{k+1}); let $s_{i\to j} > 0$ for the definiteness. Then (ii) in Lemma D5 guarantees that $\Sigma_i(s_{i\to j}, t) > 0\ \forall t \in (t_k, t_{k+1})$. So (D10) and (D13) still hold with $t_0 := t_k$. Since $\dot{s}_{i\to j}(t_k) \geq 0$ in the last equation from (D13), we arrive at a contradiction to $s_{i\to j}(t_{k+1}) = 0$. □

Corollary D4. *From any state and at any $t_0 \geq t_\dagger$, a trajectory of the considered type emerges and is extended on $[t_0, \infty)$; it visits $\mathfrak{S}_d^{\mathrm{m}}$ at most finitely many times on any finite time interval.*

Lemma D9. *Since some time, $\Sigma_i(s_i) \leq 0$ for all robots i and almost all t.*

Proof . On any interval T where the state is in $\mathfrak{S}_d^{\mathrm{sep}}$, the Danskin theorem [30] implies that $\alpha(t) := \max\left\{0, \max_i \Sigma_i(t)\right\}$ is absolutely continuous and for almost all t, we have $\dot{\alpha}(t) = 0$ if $\Sigma_i(t) \leq 0\ \forall i$; otherwise, $\dot{\alpha}(t) = \max_{i\in M(t)} \dot{\Sigma}_i(t)$, where $M(t)$ is the set of maximizers i in $\max_i \Sigma_i(t)$, and also that $\alpha(\cdot)$ has finite one-sided limits at the ends of T. Hence on any T, we have $\alpha(t) > 0 \Rightarrow \dot{\alpha}(t) \leq -\Delta_\Sigma$ by (D2), and it suffices to show that $\alpha(t_* -) \neq \alpha(t_* +) \Rightarrow \alpha(t_* -) \geq \alpha(t_* +)$. Suppose to the contrary that $\alpha(t_* -) < \alpha(t_* +)$. At $t = t_*$, there is robot i for which $\alpha(t_* +) = \Sigma_i[s_i(t_* +)] = \dot{\mathfrak{s}}_i(t_*) - \Xi[s_i(t_* +)] > \dot{\mathfrak{s}}_j(t_*) - \Xi[s_j(t_* -)]\ \forall j$. By taking $j := i$ here, we see that $s_i(t_* -) > s_i(t_* +)$. So $s_i(t_* +) = 0$ and at $t = t_*$ robot i is overtaken by a group I of robots. Hence,‘ $s_j(t_* -) = 0$, $\dot{\mathfrak{s}}_j(t_*) \geq \dot{\mathfrak{s}}_i(t_*)\ \forall j \in I$. For any such j, we have $\alpha(t_* -) \geq \dot{\mathfrak{s}}_j(t_*) - \Xi[s_j(t_* -)] = \dot{\mathfrak{s}}_j(t_*) - \Xi[0] \geq \dot{\mathfrak{s}}_i(t_*) - \Xi[0] = \alpha(t_* +)$, in violation of the starting hypothesis $\alpha(t_* -) < \alpha(t_* +)$. The contradiction obtained completes the proof. □

By combining Lemma D2 (ii) in Lemma D5, Corollary D4, and Lemma D9, we arrive at the following.

Corollary D5. *Since some time $t_\star$,* 4 *of Theorem* 2 *holds and* Γ, *and* $\dot{\mathfrak{s}}_i \equiv \Xi(s_i)$.

This and Corollary D3 show that Theorems 1 and 2 are true provided that (v) is discarded from them.

E. Proof of 5 in theorems 1 and 2.

From now on, the assumptions of 5 are adopted, and we use the enumeration from 4 in Theorem 1. We also introduce the curvilinear abscissa $\mathfrak{s}$ (the arc length) on the steady curve Γ and denote by $\mathfrak{s}_i$ the abscissa of $\boldsymbol{\varrho}_i$ counted in the counterclockwise direction. Then

$$s_i = s_{i\to i\oplus 1} = \mathfrak{s}_{i\oplus 1} - \mathfrak{s}_i, \qquad \dot{s}_{i\to j}(t) \overset{(A7)}{=} \dot{\mathfrak{s}}_j(t) - \dot{\mathfrak{s}}_i(t) \overset{\text{Corollary D5}}{=\!=\!=} \Xi[s_{j\to j\oplus 1}(t)] - \Xi[s_{i\to i\oplus 1}(t)]. \tag{E1}$$

Lemma E1. *There exists $\eta > 0$ such that $s_{i\to i\oplus 1}(t) \geq \eta\ \forall t \geq t_\star$, where $t_\star$ is taken from Corollary* D5.

Proof . The Danskin theorem [30] guarantees that $\alpha(t) := \min_i s_{i\to i\oplus 1}(t)$ is absolutely continuous and $\dot{\alpha}(t) = \min_{i\in M(t)} \dot{s}_{i\to i\oplus 1}(t)$ for almost all $t > t_\star$, where $M(t)$ is the set of minimizers i in $\min_i s_{i\to i\oplus 1}(t)$. For $i \in M(t)$ and due to (E1), we have $\dot{s}_{i\to i\oplus 1}(t) = \Xi[s_{i\oplus 1\to i\oplus 2}(t)] - \Xi[s_{i\to i\oplus 1}(t)] \geq 0$ by (20). Hence, $\dot{\alpha}(t) \geq 0$ for almost all $t \geq t_\star$ and so $\alpha(t) \geq \eta := \alpha(t_\star) > 0\ \forall t \geq t_\star$.

The *ω-limit distribution* $\mathcal{R} = [\mathfrak{r}_0, \ldots, \mathfrak{r}_{N-1}]$ is an ω-limit point of $R(t) := [\boldsymbol{\varrho}_0(t), \ldots, \boldsymbol{\varrho}_{N-1}(t)]$, that is, the limit $\lim_{j\to\infty} R(t_j)$ associated with a time sequence $t_1 < t_2 < \ldots < t_j \xrightarrow{j\to\infty} \infty$. By [31, Theorem 1.1, Chapter VII], the set $\mathfrak{R}$ of all $\mathcal{R}$'s is compact and nonempty. Let $s_{i\to j}(\mathcal{R})$ stand for the length of the counterclockwise Γ-arc from $\mathfrak{r}_i$ to $\mathfrak{r}_j$ and put $s_{\min}(\mathcal{R}) := \min_i s_{i\to i\oplus 1}(\mathcal{R})$. By Lemma E1, $s_{\min}(\mathcal{R}) > 0\ \forall \mathcal{R} \in \mathfrak{R}$. Evidently, both $s_{i\to j}(\mathcal{R})$ and $s_{\min}(\mathcal{R})$ depend on $\mathcal{R} \in \mathfrak{R}$ continuously. We recall that P is the perimeter of Γ.

Lemma E2. *The following relation holds for any robot i:* $s_{i\to i\oplus 1}(t) \to P/N \quad \text{as} \quad t \to \infty.$

Proof. The continuous map $s_{\min}(\cdot) > 0$ attains its minimum $s^-_{\min} > 0$ on the compact set $\mathfrak{R}$ at some "point" $\mathcal{R}$. We first show that $s^-_{\min} \geq P/N$. Suppose the contrary. Then, $s_{i\to i\oplus 1}(\mathcal{R}) = s^-_{\min} < P/N < \Delta^s$ for some i, where the last inequality is taken from 5 in Theorem 1. The first inequality entails that the equation cannot be true for all i. So there exists i such that $s_{i\to i\oplus 1}(\mathcal{R}) = s^-_{\min}$ and $s_{i\oplus 1\to i\oplus 2}(\mathcal{R}) > s^-_{\min} > 0$. Let $\{t_k\}_k$ be a time sequence associated with $\mathcal{E}$. Then for large enough k, we have $s_{i\to i\oplus 1}(t_k) \in (s^-_{\min} - \varepsilon, s^-_{\min} + \varepsilon)$ and $s_{i\oplus 1\to i\oplus 2}(t_k) > s^-_{\min} + 3\varepsilon$, where $\varepsilon < (\Delta^s - s^-_{\min})/3$. We invoke the constants from (20), (21), denote $\Delta t := \frac{\underline{\Xi}'\varepsilon}{8\overline{\Xi}'\overline{\Xi}}$, $t^-_k := t_k - \Delta t$ and observe that for $k \approx \infty$,

$$\begin{aligned} t \in [t^-_k, t_k] \Rightarrow \dot{s}_{i\to i\oplus 1}(t) &\overset{(E1)}{=} \Xi[s_{i\oplus 1\to i\oplus 2}(t)] - \Xi[s_{i\to i\oplus 1}(t)] = \left\{\Xi[s_{i\oplus 1\to i\oplus 2}(t_k)] - \Xi[s_{i\to i\oplus 1}(t_k)]\right\} \\ &+ \left\{\Xi[s_{i\oplus 1\to i\oplus 2}(t)] - \Xi[s_{i\oplus 1\to i\oplus 2}(t_k)]\right\} \\ &+ \left\{\Xi[s_{i\to i\oplus 1}(t_k)] - \Xi[s_{i\to i\oplus 1}(t)]\right\} \overset{(20),(21)}{\geq} \Xi(s^-_{\min} + 3\varepsilon) - \Xi(s^-_{\min} + \varepsilon) \\ &- \overline{\Xi}' \left[|s_{i\oplus 1\to i\oplus 2}(t) - s_{i\oplus 1\to i\oplus 2}(t_k)| + |s_{i\to i\oplus 1}(t) - s_{i\to i\oplus 1}(t_k)|\right] \\ &\overset{(20),(21),(E1)}{\geq} \underline{\Xi}'\varepsilon - 4\overline{\Xi}'\overline{\Xi}|t - t_k| \\ &\geq \underline{\Xi}'\varepsilon - 4\overline{\Xi}'\overline{\Xi}\Delta t = \underline{\Xi}'\varepsilon/2. \end{aligned}$$

It follows that $s_{i\to i\oplus 1}(t^-_k) \leq s_{i\to i\oplus 1}(t_k) - \underline{\Xi}'\varepsilon\Delta t/2$. By picking a convergent subsequence from $\{R(t^-_k)\}_k$ and passing to its limit, we acquire a ω-limit distribution $\mathcal{R}^-$ for which $s_{\min}(\mathcal{R}^-) < s^-_{\min}$, in violation of the definition of $s^-_{\min}$. This contradiction proves that $s^-_{\min} \geq P/N$.

Thus, $s_{i\to i\oplus 1}(\mathcal{R}) \geq P/N$ for all i and $\mathcal{R} \in \mathfrak{R}$. Meanwhile, $\sum_{i=0}^{N-1} s_{i\to i\oplus 1}(\mathcal{R}) = P$. It follows that

$$s_{i\to i\oplus 1}(\mathcal{R}) = P/N \quad \text{for all } i \text{ and } \mathcal{R} \in \mathfrak{R}. \tag{E2}$$

Now suppose that $s_{i\to i\oplus 1}(t) \not\to P/N$ for some i. Then there exists a time sequence $\{t_k\}$ such that $si \to i \oplus 1(t_k) \to \Delta s \neq P/N, t_k \to \infty$ as $k \to \infty$. Then by picking a convergent subsequence from $\{R(t_k)\}_k$ and passing to its limit, we acquire an ω-limit distribution for which (E2) fails to be true. This contradiction completes the proof. □

Proof of Theorem 2: Then theorem is immediate from Corollaries D3, D5, and Lemma E2. □

Proof of Theorem 1: Then theorem is immediate from Theorem 2. □

Cite this article: A. S. Matveev and V. V. Magerkin (2022). "Communication-free autonomous cooperative circumnavigation of unpredictable dynamic objects", Robotica **40**, 520–543. https://doi.org/10.1017/S0263574721000667